Photosensitized Singlet Oxygen Luminescence from the Protein Matrix of Zn-Substituted Myoglobin

ARTICLE *in* THE JOURNAL OF PHYSICAL CHEMISTRY A · FEBRUARY 2014

Impact Factor: 2.69 · DOI: 10.1021/jp501615h · Source: PubMed

7 AUTHORS, INCLUDING:

Sergei V Lepeshkevich
National Academy of Sciences of Belarus
20 PUBLICATIONS **125** CITATIONS
SEE PROFILE

M. V. Parkhats
National Academy of Sciences of Belarus
14 PUBLICATIONS **95** CITATIONS
SEE PROFILE

Ekaterina S Jarnikova
National Academy of Sciences of Belarus
3 PUBLICATIONS **10** CITATIONS
SEE PROFILE

Sergey A Usanov
National Academy of Sciences of Belarus
211 PUBLICATIONS **1,482** CITATIONS
SEE PROFILE

THE JOURNAL OF PHYSICAL CHEMISTRY A

Article

pubs.acs.org/JPCA

Photosensitized Singlet Oxygen Luminescence from the Protein Matrix of Zn-Substituted Myoglobin

Sergei V. Lepeshkevich,*[,†] Marina V. Parkhats,[†] Alexander S. Stasheuski,[†] Vladimir V. Britikov,[‡] Ekaterina S. Jarnikova,[†] Sergey A. Usanov,[‡] and Boris M. Dzhagarov[†]

[†]B.I. Stepanov Institute of Physics, National Academy of Sciences of Belarus, 68 Nezavisimosti Ave, Minsk 220072, Belarus

[‡]Institute of Bioorganic Chemistry, National Academy of Sciences of Belarus, 5 Academician V.F. Kuprevich Street, Minsk 220141, Belarus

Supporting Information

ABSTRACT: A nanosecond laser near-infrared spectrometer was used to study singlet oxygen ($^1O_2$) emission in a protein matrix. Myoglobin in which the intact heme is substituted by Zn-protoporphyrin IX (ZnPP) was employed. Every collision of ground state molecular oxygen with ZnPP in the excited triplet state results in $^1O_2$ generation within the protein matrix. The quantum yield of $^1O_2$ generation was found to be equal to 0.9 ± 0.1. On the average, six from every 10 $^1O_2$ molecules succeed in escaping from the protein matrix into the solvent. A kinetic model for $^1O_2$ generation within the protein matrix and for a subsequent $^1O_2$ deactivation was introduced and discussed. Rate constants for radiative and nonradiative $^1O_2$ deactivation within the protein were determined. The first-order radiative rate constant for $^1O_2$ deactivation within the protein was found to be 8.1 ± 1.3 times larger than the one in aqueous solutions, indicating the strong influence of the protein matrix on the radiative $^1O_2$ deactivation. Collisions of singlet oxygen with each protein amino acid and ZnPP were assumed to contribute independently to the observed radiative as well as nonradiative rate constants.

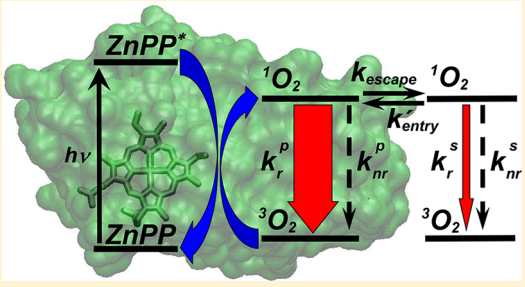

1. INTRODUCTION

Singlet oxygen ($O_2(^1\Delta_g)$ or $^1O_2$) is the lowest excited electronic state of molecular oxygen (O_2). The singlet state $^1\Delta_g$ lies closely above the $^3\Sigma_g^-$ triplet ground state. Transitions between these states are strictly forbidden for the isolated molecular oxygen by selection rules for electric dipole radiation.[1] Intermolecular interactions lead to a strong enhancement of $^1\Delta_g \rightarrow {}^3\Sigma_g^-$ emission in the gas and condensed phases.[1−3] The most common method of $^1O_2$ generation is photosensitization wherein the energy of a sensitizer excited state, which is formed by an absorption of light, is transferred to the electronic ground state of molecular oxygen.[1,3] For the most organic sensitizers, the relevant excited state is the lowest triplet. Singlet oxygen is a highly reactive species playing a significant role in chemical and biological systems, including events that result in cell death. Many of these processes involve a reaction between singlet oxygen and a given amino acid in a protein. It is well-established that protein properties can be changed upon reaction with singlet oxygen, either as a result of a structural alteration and/or a direct chemical modification. Conversely, the behavior of singlet oxygen depends on a protein structure.[4] Little is known about rate constants for reactions between singlet oxygen and quenchers when the latter are in a protein. Mainly, quenching of $^1O_2$ generated and distributed homogeneously in a solvent surrounding a protein has been studied.[4] From these experiments, the magnitude of the overall rate constant for protein-mediated $^1O_2$ removal was found to reflect the sum of rate constants for $^1O_2$ interaction with individual amino acids in a given protein. The rate constant for $^1O_2$ reaction with an amino acid depends significantly on the position of this quencher in the protein.[4] A local protein environment can either inhibit or accelerate the $^1O_2$ quenching appreciably by perturbing the electronic distribution in amino acids and increasing the local viscosity.[4] It should be stressed that photosensitized singlet oxygen production inside a protein has been studied as well.[5−7] However, $^1O_2$ deactivation within a protein matrix has not been explored in detail. Therefore, the aim of the present study was to investigate radiative as well as nonradiative $^1O_2$ deactivation within a protein matrix.

Our approach to quantify the rate constants for $^1O_2$ deactivation within a protein matrix is to generate a population of singlet oxygen within the protein matrix using a photosensitizer buried deep inside the protein. Myoglobin was chosen as the protein for this study because of its intrinsic importance in oxygen transport as well as the wealth of structural information available. Myoglobin consists of a single polypeptide chain to which heme (Fe-protoporphyrin IX) is covalently attached (Figure 1). This chain is folded to form an ellipsoid with dimensions of about 43 Å × 35 Å × 23 Å.[8] The

Received: February 14, 2014
Revised: February 19, 2014
Published: February 19, 2014

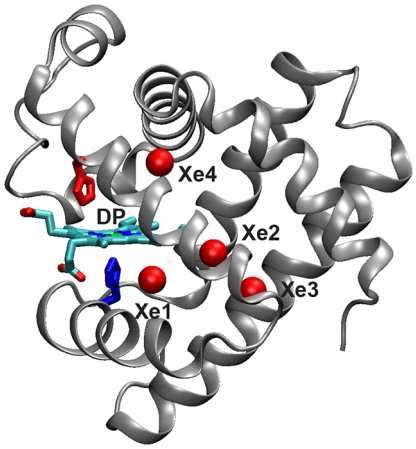

Figure 1. Structure of myoglobin showing the heme and the locations of Xe sites (PDB code 2W6W). The locations of bound Xe are represented by labeled red spheres. The location of the distal heme pocket is labeled as DP. Backbone is drawn as silver ribbons. Amino acid side chains drawn as colored sticks mark the following residues: His64 (red) and His93 (blue). The heme group is depicted in sticks.

heme group is located in a crevice in the polypeptide structure. The highly polar propionate side chains of the heme are on the surface of the protein. The rest of the heme is inside the protein. The iron atom of the heme is directly bonded to the proximal histidine (His93) (Figure 1). On the other side of the heme plane (distal side), molecular oxygen can reversibly bind to the heme iron. For many years, myoglobin has played a central role in research on ligand binding and migration inside proteins.[9−12] Time-resolved spectroscopic measurements of myoglobin photoproducts have revealed a complex ligand rebinding reaction with multiple kinetic intermediates.[10] It is commonly accepted that after photoinduced dissociation from the heme iron atom, a free ligand molecule can either escape into the solvent or rebind internally from the protein matrix. Such a reaction is referred to as geminate recombination. For those myoglobin molecules from which ligand molecules succeed in escaping into the surrounding medium, rebinding is a bimolecular reaction. Using various computational and experimental techniques,[13−15] ligand escape routes have been clearly identified in myoglobin. Four docking sites are observed[13] (Figure 1): so-called Xe4 on the distal side of the heme, Xe1 on its proximal side, Xe2 close to Xe1, and Xe3 near the surface of the protein. It has been clearly indicated[16−18] that these sites, especially Xe4 and Xe1, are involved in the ligand migration pathways. Moreover, ligand entry and exit from myoglobin occur mainly through the distal histidine (His64) gate located between the distal pocket and solvent (Figure 1).[11]

It should be stressed that the heme buried inside the protein cannot generate singlet oxygen since lifetimes of excited-states of the oxy- and deoxyheme are short enough (no more than a few picoseconds[19]) to preclude, in a bimolecular reaction, an energy transfer from the excited states of the heme to the ground state molecular oxygen. Moreover, photodissociation of molecular oxygen from the heme iron does not produce detectable quantities of singlet oxygen.[20] In the present study, to create an intrinsic photosensitizer and not significantly alter the structure and stability of the protein as well as not substantially affect the structural fluctuations that permit the O_2 migration,[21−24] the heme iron was replaced with zinc. Thus, we employed myoglobin in which the intact heme is substituted by Zn-protoporphyrin IX (ZnPP), whose the lowest excited triplet state is long-lived enough to generate singlet oxygen. Using the photosensitizer buried deep inside the protein, we determined for the first time the rate constants for radiative as well as nonradiative $^1O_2$ deactivation within the protein matrix. To find the deactivation rate constants, rate constants for $^1O_2$ escape from and entry into Zn-substituted myoglobin were evaluated from laser flash photolysis studies of the O_2 rebinding to ferrous myoglobin.

2. EXPERIMENTAL SECTION

2.1. Materials. ZnPP and horse heart metmyoglobin were purchased from Sigma. Metmyoglobin was of the highest purity available and was used as received. The tosylate salt of 5,10,15,20-tetrakis (4-*N*-methylpyridyl) porphyrin, TMPyP, was a gift from Dr. V.L. Malinovskii. Zn(II) meso-tetraphenylporphyrin (ZnTPP) was a gift from A. M. Shulga.

2.2. Preparation of Oxymyoglobin. Oxymyoglobin was obtained by the method described elsewhere.[19] The concentration of oxymyoglobin was determined by measurement of absorbance at 542 and 580 nm, the molar extinction coefficient being taken as 13.9×10^3 and 14.4×10^3 ($cm^{-1}{\cdot}M^{-1}$), respectively.[25] For O_2 rebinding measurements, oxymyoglobin at a concentration of 20 μM was prepared in 50 mM citrate-phosphate buffer (pH 4.5, 4.9, and 7.4) at 18 °C. To convert O_2 partial pressures to molarities of dissolved O_2, the solubility coefficient of 1.87 $\mu M{\cdot}mmHg^{-1}$ was used.

2.3. Preparation of Apomyoglobin. To prepare the apoform of myoglobin, the heme was removed from myoglobin by the acid-butanone method.[26] Briefly, after the pH of the myoglobin solution was lowered to ca. 2.5, an equivolume of 2-butanone was added to the solution to extract the heme. The mixture was shaken until a formation of a lower hazy pale-yellow protein layer and an upper dark-brown heme-containing layer. The upper layer containing the extracted heme was discarded. The procedure was repeated twice to ensure complete removal of the heme. The aqueous apoprotein solution (ca. 50 mL) was then dialyzed twice for 8 h against 2 L of 0.1 M potassium-phosphate buffer, pH 7.2. The whole procedure was carried out at 4 °C away from the direct light.

2.4. Reconstitution of Apomyoglobin with ZnPP. To reconstitute ZnPP into apomyoglobin, approximately 5 mg of ZnPP was dissolved in 1 mL of dimethyl formamide and added dropwise to the apomyoglobin solution with gentle stirring. The mixture was kept in the dark for 3 h. The obtained solution was loaded onto a Sephadex G25 column, equilibrated with 0.1 M Tris-HCl buffer, pH 7.2, to remove free porphyrin. The purified solution of Zn-substituted myoglobin was concentrated on a hydroxyapatite column, equilibrated with 0.1 M Tris-HCl buffer, pH 7.2, 20% (w/v) glycerol. Subsequently, Zn-substituted myoglobin was eluted with 0.5 M potassium-phosphate buffer, pH 7.2, 20% (w/v) glycerol and stored at −20 °C until use. The whole procedure was carried out at 4 °C away from the direct light. Before measurements, the samples were passed through a small Sephadex G-25 column to remove possible denatured protein. The quality and homogeneity of the final product was investigated using absorption and emission spectroscopy. The concentration of Zn-substituted myoglobin was determined by measurement of absorbance at 554 nm, the molar extinction coefficient being taken as 10.4×10^3 ($cm^{-1}{\cdot}M^{-1}$).[27] For experiments, Zn-substituted myoglobin was prepared in 50 mM citrate-phosphate buffer, pH 4.9 and 7.4, at 18 °C, using a cuvette with continuous magnetic stirring. The

dx.doi.org/10.1021/jp501615h | J. Phys. Chem. A 2014, 118, 1864−1878

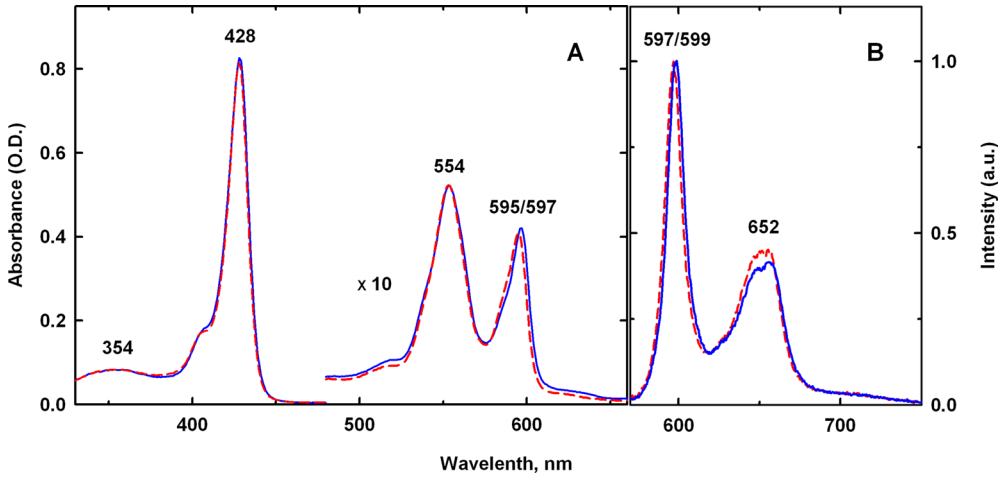

Figure 2. Optical properties of Zn-substituted myoglobin. Absorption (A) and normalized fluorescence spectra (B). Protein concentration, 50 μM (A) and 13 μM (B). Conditions: 50 mM citrate-phosphate buffer, pH 7.4 (solid blue lines) and pH 4.9 (dashed red lines), at 18 °C. Absorption was recorded with a UV−vis spectrophotometer. The fluorescence spectra were selectively excited with a lamp at 552 nm.

acidic unstability of Zn-substituted myoglobin prevents performing experiments at lower pH.

2.5. Steady-State Absorption and Fluorescence Measurements. Absorption spectra were recorded on a spectrophotometer (Proscan Special Instruments, MC 122, Belarus) in quartz cuvettes. Fluorescence spectra corrected for the spectral response of the detection system were recorded on a spectrofluorimeter[28] using the excitation wavelength of 552 nm. The fluorescence quantum yield φ was determined by a relative method using a solution of ZnTPP in toluene as a fluorescent standard, for which the quantum yield of 0.03 was obtained.[29] The relative accuracy in determination of the fluorescence quantum yield was 5%.

2.6. Time-Resolved Fluorescence Measurements. The lifetime of the excited singlet state, τ_s, of Zn-substituted myoglobin was determined by measuring fluorescence decays using a modified PRA-3000 pulse fluorometer (Photochemical Research Associates, London, Ontario, Canada) operating in the time-correlated single photon counting mode. The decays were analyzed by means of Edinburgh FLA900 software. The lifetime of the excited singlet state was determined by the nonlinear least-squares reconvolution analysis of fluorescence decay curves assuming a single-exponential fluorescence decay law $F(t) = F(0)\exp(-t/\tau_s)$. The estimated relative errors in fluorescence lifetimes were about 5%. The excitation source was a 408-nm pulsed light-emitting diode (PLS-410, PicoQuant GmbH), full width at half-maximum (fwhm) of the diode pulses being ~990 ps.

2.7. Time-Resolved Spectroscopy. Kinetics of the triplet−triplet absorption as well as kinetics for the O_2 rebinding to myoglobin were measured on a nanosecond laser spectrometer.[30−33] The second harmonic of a 8 ns Nd:YAG laser (LS-2132U, LOTIS TII, Belarus) at 532 nm was used for photoexcitation. Typical energies of the laser pulses used for triplet−triplet absorption, geminate and bimolecular O_2 rebinding measurements are 0.5, 2, and 25 mJ, respectively. A halogen lamp KGM24−150 (Brest Lamp Plant, Belarus) was used as a probing light source. A FEU-84 photomultiplier tube was applied as a light detector. The output of the photodetector (photoinduced current) was digitized by an oscilloscope BORDO110 (Unitechprom BSU, Belarus). After the sample was excited by the laser pulse, the change in photoinduced current, $\Delta I(t)$, was measured. Due to the finite duration of both the excitation pulse and response of the detection electronics, $\Delta I(t)$ is in fact the convolution of (i) the apparatus response function, $R(t)$, determined by the laser pulse shape as well as the time response of the detection system with (ii) a function, which is proportional to the change in transmitted probe light intensity after the laser excitation:

$$\Delta I(t) = I_0 \cdot \int_0^t R(t - t') \cdot (10^{-\Delta A(t')} - 1)\, dt' \quad (1)$$

where I_0 is the photoinduced current before the laser shot; $\Delta A(t)$ is the change in sample absorbance. In the limit where $R(t)$ is short compared with $\Delta A(t)$, eq 1 takes the following form:

$$\Delta A(t) = -\lg\left(1 + \frac{\Delta I(t)}{I_0}\right) \quad (2)$$

The apparatus response function $R(t)$ was taken into account for nanosecond data analysis. In this case, eq 1 was used. On the other hand, for microsecond data fitting, eq 2 was applied.

Triplet−Triplet Absorption Measurements. Kinetics of the triplet−triplet absorption of Zn-substituted myoglobin was examined in the microsecond time range. Transient absorption changes were monitored at 460 nm. The kinetics was fitted by an exponential function: $\Delta A(t) = A_0 \exp(-t/\tau_T)$, where $\Delta A(t)$ is the change in sample absorbance, and A_0 is the amplitude of the light-induced absorption changes at zero time.

Measurements of O_2 Rebinding to Myoglobin. The O_2 rebinding to myoglobin was examined using a previously described methodology.[32] Briefly, transient absorption changes were monitored in the Soret band (430 nm). The change in the absorbance of an oxygenated sample after photodissociation is in direct proportion to the number of photodissociated O_2 molecules. The number of photodissociated O_2 molecules to that of absorbed light quanta defines the primary quantum yield of photodissociation, γ_0. In their turn, the number of O_2 molecules which escape from the protein matrix after photodissociation to that of absorbed light quanta defines the quantum yield of bimolecular recombination, γ. The quantum yield γ for myoglobin was determined using a relative method described previously.[34] Human hemoglobin in 10 mM Tris HCl

dx.doi.org/10.1021/jp501615h | J. Phys. Chem. A 2014, 118, 1864−1878

buffer, pH 7.4, was used as a reference standard, for which γ = 0.023 ± 0.003 was obtained.[33]

2.8. Time-Resolved Singlet Oxygen Detection. Time-resolved luminescence in the near-infrared region (NIR) was measured on a nanosecond laser NIR spectrometer.[20] Samples were excited by the second harmonic (532 nm) of a Nd:YAG laser (DTL-314QT, Laser-export Co. Ltd.). Typical parameters of the laser were as follows: the pulse width of 10 ns, the pulse energy of 1 μJ, and the repetition rate of 2.5 kHz. Luminescence radiation, collected with a high-throughput optical system, was spectrally isolated with bandpass filters (less than 13 nm fwhm) (Thorlabs GmbH; Axicon) and directed to a photomultiplier tube, PMT (model H10330A-45, Hamamatsu Photonics K.K.), operated in the photon-counting mode. After amplification by 1.6 GHz HFAC-26 unit (Becker & Hickl GmbH), the output of the PMT was sent to a multiscaler (P7888-2, FAST ComTec GmbH). The time channel width of the multiscaler was set to 32 ns.

3. RESULTS AND DISCUSSION

3.1. Photophysical Properties of Zn-Substituted Myoglobin. UV−vis absorption and fluorescence spectra of Zn-substituted myoglobin in the buffer solutions are plotted in Figure 2 (panels A and B, respectively). The present spectra were recorded at pH 4.9 (dashed red lines) and pH 7.4 (solid blue lines). The absorption spectrum at pH 7.4 is characterized by a strong Soret band with the maximum at 428 nm and weaker Q(1,0) and Q(0,0) bands at 554 and 597 nm, respectively. The fluorescence Q(0,0) and Q(0,1) bands are at 599 and 652 nm, respectively. The absorption and fluorescence spectra are similar to those published in the literature.[35,36] As it is seen from Figure 2, the absorption and fluorescence spectra are only slightly sensitive to pH. In agreement with previous results,[24] a blue-shift of Q(0,0) electronic absorption and fluorescence bands by 2 nm is observed upon lowering the pH from 7.4 to 4.9.

Using the time-resolved fluorescence technique, we found that, within the experimental accuracy, the lifetime of the excited singlet state, τ_s, of Zn-substituted myoglobin does not depend on proton concentration, the lifetime τ_s being equal to 2.3 ns and similar to those published in the literature.[36,37] Moreover, steady-state fluorescence measurements showed that the fluorescence quantum yield φ is constant as well, its value being equal to 0.03. All the above-mentioned spectral and kinetic features are typical of the ZnPP monomer being bound firmly into the heme pocket of apomyoglobin.

3.2. Triplet State of Zn-Substituted Myoglobin. *Triplet Quantum Yield.* Porphyrins with the central Zn^{2+} ion in the porphyrin ring are capable of binding only one extra-ligand. In Zn-substituted myoglobin, the proximal histidine (His93) is coordinated to ZnPP. The extra-ligation by histidine is due to the interaction of the unshared electron pair of ligand nitrogen with empty d-orbitals of porphyrin Zn^{2+} ion. Extra-ligation effects for various monomeric Zn-porphyrins have been well documented.[38] It has been shown[38] that the extra-ligation does not influence essentially on the fluorescence quantum yield φ. It means that additional nonradiative deactivation processes of the singlet excited state are not enhanced in the liganded Zn-porphyrins. Thus, the quantum yield for singlet to triplet intersystem crossing, i.e., the triplet quantum yield Q_T, is not changed appreciably. Therefore, the triplet quantum yield of Zn-substituted myoglobin can be considered to be equal to those of monomeric Zn-porphyrins. The triplet quantum yields of various monomeric Zn-porphyrins typically lie in the range between 0.85 and 0.95.[39−41] Consequently, the intermediate value, Q_T = 0.90 ± 0.05, can be taken as the triplet quantum yields of Zn-substituted myoglobin and will be used in the following discussion.

Triplet−Triplet Absorption. The triplet state lifetime, τ_T, of porphyrin-related compounds in a homogeneous medium is well-known to be strongly dependent on the concentration of dissolved molecular oxygen, $[O_2]$:

$$1/\tau_T = 1/\tau_{T0} + k_q(D)[O_2] \quad (3)$$

where τ_{T0} is the triplet state lifetime in an oxygen-free medium, and k_q is the medium-dependent bimolecular rate constant of triplet state quenching by molecular oxygen. The reciprocal value of τ_T is the rate constant for triplet state deactivation, k_T. In view of the quenching of the excited triplet state of ZnPP in myoglobin, eq 3 can be applied by utilizing the concentration of ground state molecular oxygen in the surrounding medium or within the protein matrix. Obviously, in these two cases, the bimolecular rate constant in eq 3 has two different meanings. In the first case, when the concentration of molecular oxygen dissolved in the surrounding medium is utilized, the rate constant, hereafter denoted as the bimolecular quenching constant for Zn-substituted myoglobin, k_q^p, characterizes the quenching of the excited triplet state of buried ZnPP by molecular oxygen dissolved in the medium surrounding the protein matrix. In the second case, when the concentration of molecular oxygen within the protein matrix is utilized, the rate constant characterizes the triplet state quenching by molecular oxygen within the protein matrix. To calculate the bimolecular quenching constant k_q^p, eq 3 will be applied by us in this section. To describe in detail the triplet state quenching by molecular oxygen within the protein matrix, eq 3 will be rewritten in Section 3.6 (eq 20).

The most probable direct product of the triplet state quenching is singlet oxygen, which is well-known to react readily with porphyrins as well as protein amino acids. Upon repeated photolysis of Zn-substituted myoglobin in the presence of molecular oxygen, the Soret band absorption (not shown) as well as the amplitude of the light-induced triplet−triplet absorption changes, A_0 (Supporting Information Figure S1A), are decreased, indicating destruction of the porphyrin chromophore and/or protein denaturation. Moreover, during the successive irradiation, molecular oxygen is consumed. To preclude measurable changes in the O_2 concentration, the protein concentration (10 μM) was chosen to be substantially less than the one of dissolved molecular oxygen (300 μM). At the chosen protein concentration, the triplet state lifetime, τ_T, does not change during the successive irradiation (Supporting Information Figure S1B), indicating that a measurable depletion of molecular oxygen does not occur. These conditions were used to correctly determine the rate constant for triplet state deactivation in air-saturated buffers, k_T. Typical kinetics of the triplet−triplet absorption of Zn-substituted myoglobin is shown in Figure 3. The triplet state lifetime was found to be constant and equal to τ_T = 24 ± 2 μs at pH 7.4 and 4.9. The rate constant k_T is equal to (42 ± 3) × 10^3 s^{-1}. In oxygen-free buffer solutions, the triplet state lifetime τ_{T0} of Zn-substituted myoglobin is ∼14 ms (ref 42) being more than 2 orders of magnitude larger than the value of τ_T. Subsequently, using eq 3, the bimolecular quenching rate constant for Zn-substituted myoglobin, k_q^p, was found to be (1.4 ± 0.1)·10^8 $M^{-1}\cdot s^{-1}$. This value obtained for horse heart

dx.doi.org/10.1021/jp501615h | J. Phys. Chem. A 2014, 118, 1864−1878

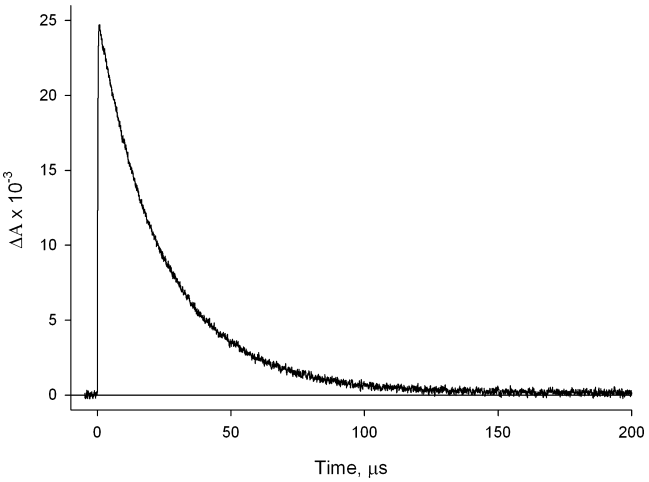

Figure 3. Kinetics of the triplet−triplet absorption of Zn-substituted myoglobin. The reported kinetics data are the average of 380 shots. Concentration of Zn-substituted myoglobin, 10 μM. Conditions: 50 mM citrate-phosphate buffer, pH 7.4, at 18 °C. Excitation wavelength, λ_{exc} = 532 nm; detection wavelength, λ_{det} = 460 nm ($\Delta\lambda$ = 10 nm).

myoglobin is in excellent agreement with earlier published values for sperm whale myoglobin.[42,43]

It should be stressed that the bimolecular quenching constant k_q (eq 3) is representative of the rate constant for quencher diffusion toward the excited porphyrin.[44] The quenching of the excited triplet state of ZnPP in aqueous solutions and in myoglobin are directly proportional to the diffusion constants for ground state molecular oxygen in the aqueous solutions, D_s, and in the protein matrix, D_p, respectively. Here, the indices "s" and "p" denote the solution and protein phases, respectively. According to Barboy et al.,[44] using the calculated bimolecular quenching constant for Zn-substituted myoglobin, k_q^p, and the one for monomeric ZnPP in the aqueous solutions, k_q^s, the ratio of D_s to D_p can be determined: $D_s/D_p = k_q^s/k_q^p$. The value, $k_q^s = (1.2 \pm 0.2) \times 10^9$ $M^{-1}\cdot s^{-1}$,[39,43] can be taken as the quenching constant for ZnPP in the aqueous solutions. Hence, the ratio D_s/D_p was found to be equal to 8.6 ± 0.3. It is reasonable to assume that, in a given medium, the diffusion constant for ground state molecular oxygen is the same as that for singlet oxygen. Based on this assumption, the found ratio of the diffusion constants will be used in Section 3.7 to compare the rate constants of $^1O_2$ quenching by amino acids in the aqueous solutions and in Zn-substituted myoglobin. Moreover, we assumed that the O_2 migration within Zn-substituted myoglobin is similar to that observed in ferrous native myoglobin. The replacement of the heme iron with zinc does not significantly alter the structure and stability of myoglobin as well as not substantially affect the structural fluctuations that permit the O_2 migration.[21−24] Therefore, rate constants for the migration of ground state molecular oxygen as well as singlet oxygen in Zn-substituted myoglobin can be considered to be equal to the corresponding rate constants for the O_2 migration in ferrous myoglobin and can be evaluated from laser flash photolysis studies of the O_2 rebinding to ferrous myoglobin.

3.3. Bimolecular and Geminate O_2 Rebinding to Ferrous Myoglobin. Typical kinetics for the ground state molecular oxygen rebinding to ferrous myoglobin after the photoinduced dissociation from the heme iron atom are shown in Figure 4. The initial rebinding occurring throughout the nanosecond time range (Figure 4A) has been identified as the

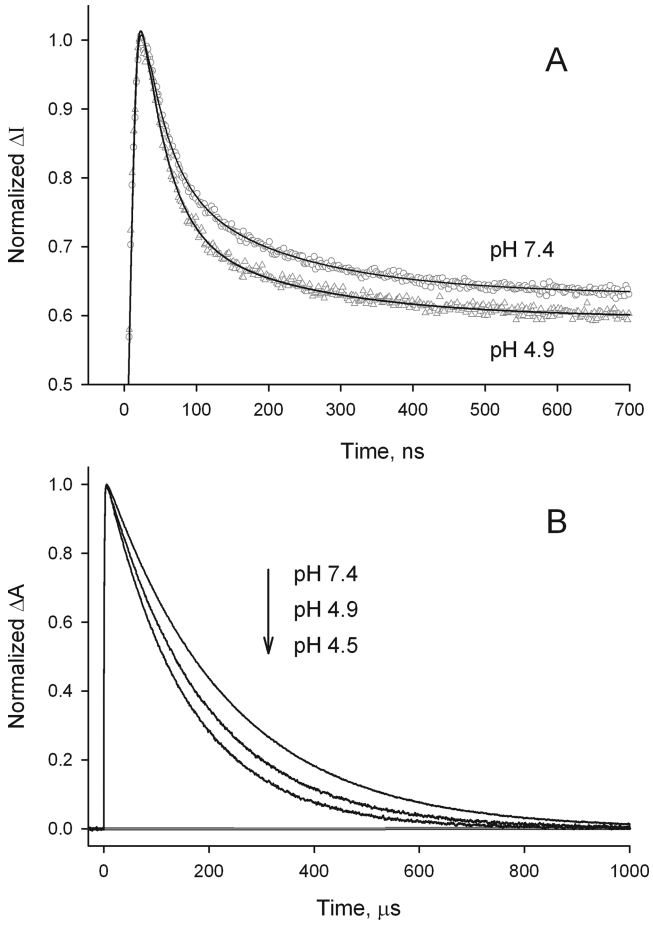

Figure 4. Normalized oxygen rebinding kinetics for horse heart myoglobin in buffer solutions at pH 7.4, 4.9, and 4.5. (A and B) Normalized kinetics for the geminate (A) and bimolecular O_2 rebinding to myoglobin (B). The normalized kinetics for the geminate O_2 rebinding at pH 4.9 coincides with the one at pH 4.5 (not shown). Conditions: 50 mM citrate-phosphate buffer, at 18 °C. Myoglobin concentration is 20 μM. Excitation wavelength, λ_{exc} = 532 nm; detection wavelength, λ_{det} = 430 nm ($\Delta\lambda$ = 10 nm). The observed maximal changes in the optical density of the sample are 0.06 OD (A) and 0.015 OD (B). In panel A, symbols correspond to experimental data, and the solid lines show data fit. In panel B, the solid lines correspond to experimental data.

O_2 rebinding from within the protein matrix (geminate recombination). The slow phase, observed in the microsecond time range (Figure 4B), corresponds to the bimolecular O_2 rebinding from solvent. The kinetics of bimolecular rebinding was studied under pseudo-first order conditions. The normalized kinetics of bimolecular oxygenation (Figure 4B) was fitted with an exponential function:

$$\Delta A_{norm}^{\mu s}(t) = e^{-k'\cdot[O_2]\cdot t} \quad (4)$$

where the superscript "μs" corresponds to experimental data obtained for the microsecond time range; $\Delta A_{norm}^{\mu s}(t)$ is the normalized change in sample absorbance, and k' is the rate constant for the bimolecular O_2 rebinding to myoglobin. The bimolecular association rate constant, k', and the quantum yield of bimolecular recombination, γ, measured in the pH range from 7.4 to 4.5 are given in Table 1. As it is seen, the decrease in pH from 7.4 to 4.5 results in an increase by a factor of 1.53 ± 0.05 in the bimolecular association rate constant k'. The

dx.doi.org/10.1021/jp501615h | J. Phys. Chem. A 2014, 118, 1864−1878

Table 1. Parameters for O_2 Rebinding to Ferrous Myoglobin

pH	k' ($\mu M^{-1}\cdot s^{-1}$)	$\gamma \times 10^{-2}$	$\gamma_0 \times 10^{-2}$	τ_1 (ns)	τ_2 (ns)	a_1 (%)	a_2 (%)	a_{const} (%)
7.4	15.0 ± 0.4	12 ± 2	23 ± 3	33 ± 2	174 ± 7	32 ± 1	16 ± 1	52 ± 1
4.9	19.0 ± 0.7	10 ± 2	21 ± 3	34 ± 2	187 ± 12	40 ± 1	12 ± 1	48 ± 1
4.5	22.9 ± 0.5	10 ± 2	21 ± 3	35 ± 3	177 ± 17	41 ± 1	11 ± 1	48 ± 1

Myoglobin concentration is 20 μM. Conditions: 50 mM citrate-phosphate buffer, at 18 °C. The uncertainties are presented as 95% confidence intervals.

Scheme 1. Four-State Kinetic, Side Path Model for O_2 Dissociation, Migration, and Rebinding in Ferrous Myoglobin

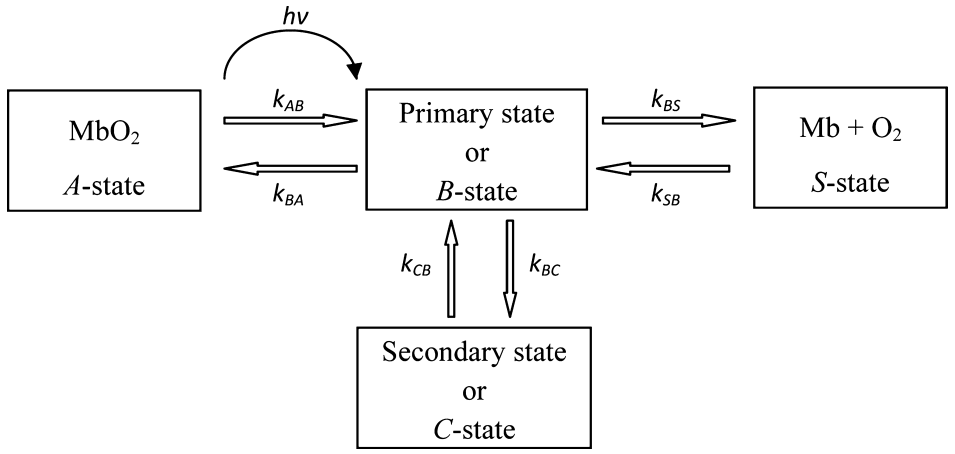

Table 2. Geminate Rate Constants for O_2 Rebinding to Ferrous Myoglobin

pH	k_{BA} (μs^{-1})	k_{BS} (μs^{-1})	k_{SB} ($\mu M^{-1}\cdot s^{-1}$)	k_{BC} (μs^{-1})	k_{CB} (μs^{-1})	$K_{SB}{}^a$ (M^{-1})
7.4	10.6 ± 0.7	11.5 ± 0.7	31.3 ± 1.1	6.1 ± 0.6	7.9 ± 0.3	2.7 ± 0.2
4.9	12.4 ± 0.8	11.5 ± 0.7	36.5 ± 1.5	4.3 ± 0.5	6.6 ± 0.4	3.2 ± 0.2
4.5	12.3 ± 1.0	11.4 ± 1.0	44.0 ± 1.3	3.7 ± 0.6	6.8 ± 0.6	3.9 ± 0.3

Myoglobin concentration is 20 μM. Conditions: 50 mM citrate-phosphate buffer, at 18 °C. The uncertainties are presented as 95% confidence intervals. [a]The equilibrium constant for O_2 entry into myoglobin, K_{SB}, was calculated as k_{SB}/k_{BS}.

quantum yield of bimolecular recombination, γ, within the accuracy of the measurements, does not change.

In turn, the kinetic traces in the nanosecond time range (Figure 4A) can be fitted by the sum of two exponential terms and an offset:

$$\Delta A^{ns}_{norm}(t) = a_1 e^{-t/\tau_1} + a_2 e^{-t/\tau_2} + a_{const} \quad (5)$$

where the superscript "ns" corresponds to experimental data obtained for the nanosecond time range; $\Delta A^{ns}_{norm}(t)$ is the normalized change in sample absorbance; a_i and τ_i (i = 1,2) are the amplitudes and decay times of the kinetic components, respectively; a_{const} is the offset reflecting (i) the amount of O_2 molecules that escape from the protein into the solvent after the photodissociation and, obviously, (ii) the amount of photodeoxygenated myoglobin molecules that rebind molecular oxygen from the solvent with the bimolecular rate constant k'. Table 1 lists the results of approximation by eqs 1 and 5. In myoglobin, a_{const} (eq 5) relates to the efficiency of O_2 escape from the protein matrix into the environmental medium after photodissociation. Based on the calculated value of a_{const}, the primary quantum yield of photodissociation, γ_0, was determined (Table 1) using the formula: $\gamma_0 = \gamma/a_{const}$,[34] where γ is the quantum yield of bimolecular recombination. The primary quantum yield γ_0 measured by us agree well with those previously reported for myoglobin[45] and hemoglobin.[46]

The obtained geminate data can be represented by any scheme that reduces to two exponential decays (eq 5). We followed a scheme proposed for myoglobin to describe the O_2 rebinding kinetics with a simplified three-step, side path model (Scheme 1).[9,11,47] It is considered that molecular oxygen enters the protein through the histidine gate (Scheme 1; S → B). The ligand is then captured in the distal pocket (Figure 1) above pyrrole rings B and C in the space circumscribed by His64, Val68, Phe43, Leu29, Leu32, and Ile107. Ligands in this location are designated as being in state "B", which is the primary docking site.[11,12,14−18,47] The ligand can then move further into the protein (Scheme 1; B → C), bind to the heme iron atom (B → A), or exit the protein back through the histidine gate (B → S). The rate constants for O_2 intraprotein rebinding, escape from within the primary docking site into the environmental medium, and movement through the protein can be expressed through the empirical kinetic parameters a_i and τ_i (i = 1,2) of the geminate components (eq 5) by analytical solution of the system of coupled differential equations for the side path model. The details of this procedure are described in the Supporting Information. Sets of the calculated geminate rate constants are given in Table 2. Assuming that the O_2 migration in ferrous myoglobin is similar to that of $^1O_2$ in Zn-substituted myoglobin, the calculated geminate rate constants provide a basis for an obtaining the bimolecular rate constant for $^1O_2$ entry into, k'_{entry}, and the first-order rate constant for $^1O_2$ escape from Zn-substituted myoglobin, k_{escape}, in the limit when singlet oxygen does not react with the protein.

dx.doi.org/10.1021/jp501615h | J. Phys. Chem. A 2014, 118, 1864−1878

3.4. Rate Constants for $^1O_2$ Entry into and Escape from Zn-Substituted Myoglobin. To find the rate constants k'_{entry} and k_{escape}, the proper kinetic model for $^1O_2$ migration (Scheme 2) was chosen. Scheme 2 is a modified version of the

Scheme 2. Two-State Model for $^1O_2$ Migration

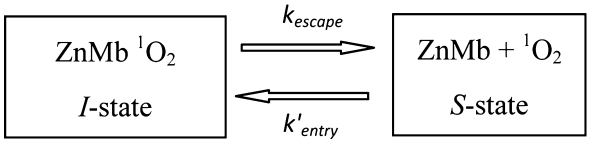

above-mentioned kinetic model for O_2 dissociation, migration, and rebinding in ferrous myoglobin (Scheme 1). In Scheme 2, the ligand-bound state (A-state) is absent, since Zn-substituted myoglobin does not covalently bind molecular oxygen. Moreover, B and C-states defined in Scheme 1 is considered in Scheme 2 as a single state, hereafter called the interior state (I-state). The rate constants k'_{entry} and k_{escape} for Scheme 2 can be expressed through the rate constants for Scheme 1:

$$k'_{entry} = k_{SB} \tag{6}$$

$$k_{escape} = \frac{k_{BS} \cdot k_{CB}}{k_{CB} + k_{BC}} \tag{7}$$

Additionally, the equilibrium constant for $^1O_2$ entry into Zn-substituted myoglobin was determined as $K_{entry} = k'_{entry}/k_{escape}$. The rate constants k'_{entry} and k_{escape} as well as the equilibrium constant K_{entry} were calculated and listed in Table 3.

Table 3. Rate Constants for $^1O_2$ Entry into and Escape from Zn-Substituted Myoglobin

pH	k'_{entry} ($\mu M^{-1}\cdot s^{-1}$)	k_{escape} (μs^{-1})	$K_{entry} = k'_{entry}/k_{escape}$ (M^{-1})
7.4	31.3 ± 1.1	6.5 ± 0.5	4.8 ± 0.4
4.9	36.5 ± 1.5	6.9 ± 0.6	5.3 ± 0.5
4.5	44.0 ± 1.3	7.4 ± 0.9	6.0 ± 0.7

The uncertainties are presented as 95% confidence intervals.

3.5. Luminescence Emitted by $^1O_2$ Photosensitized by a Standard. The direct detection of $^1O_2$ generated by Zn-substituted myoglobin was performed by measuring $^1O_2$ luminescence at 1270 nm. The light emission at 1270 nm corresponds to the $^1O_2$ monomolecular decay ($^1\Delta_g \rightarrow {}^3\Sigma_g^-$). To quantify the $^1O_2$ generation, the estimated intensity of $^1O_2$ luminescence was compared with the one emitted by $^1O_2$ generated by a known standard, namely, the highly effective water-soluble cationic photosensitizer TMPyP[48] (for further details of the comparison, see the following sections). The experimentally measured time-dependent intensity for the standard, $S_{st}(t)$, as well as for any photosensitizer in a homogeneous medium, is proportional to the photosensitized $^1O_2$ concentration, $[^1O_2^{st}](t)$:

$$S_{st}(t) = \frac{\kappa}{n^2} k_r^s [^1O_2^{st}](t) \tag{8}$$

where κ is a proportionality constant that contains geometrical and electronic factors of the detection system, n is the refractive index of solvent, and k_r^s is the rate constant of solvent-dependent $^1O_2$ radiative decay. In their turn, the time dependence of photosensitized $^1O_2$ concentration is given by

$$[^1O_2^{st}](t) = \frac{k_{T\Delta}^{st}[O_2][T_1]_{t=0}^{st}}{k_T^{st} - k_\Delta}(e^{-k_\Delta t} - e^{-k_T^{st} t}) \tag{9}$$

where $k_{T\Delta}^{st}$ is the rate constant of energy transfer between the excited triplet state of the standard and the ground state molecular oxygen, resulting in $^1O_2$ production. $[T_1]_{t=0}^{st}$ is the initial concentration of the sensitizer triplet state T_1. k_T^{st} is the rate constant for sensitizer triplet state deactivation; k_Δ is the rate constant for $^1O_2$ deactivation in water. Symbols used frequently in this paper are summarized in Table 4. Equation 9 is true in the case of a homogeneous environment, low laser energy, delta pulse excitation, and when there is no back transfer of energy from singlet oxygen to the photosensitizer triplet state.[49] All these conditions are fulfilled for experiments with the standard.

Upon integrating eq 9 with respect to the time, one can obtain the integral intensity of luminescence emitted by photosensitized $^1O_2$, generated by the standard

$$I_{st} = \frac{\kappa}{n^2} \frac{k_r^s k_{T\Delta}^{st}[O_2][T_1]_{t=0}^{st}}{k_\Delta k_T^{st}} \tag{10}$$

A time-resolved $^1O_2$ luminescence trace, generated by photoexcitation of photosensitizer TMPyP in an air-saturated aqueous solution, is shown in Figure 5A (symbols). The $^1O_2$ generation was confirmed by spectral analysis of the light emission and by the quenching effect of sodium azide (not shown). Taking into account eqs 8 and 9, the experimentally measured time-dependent intensity of luminescence emitted by $^1O_2$ photosensitized by the standard was fitted with the following function:

$$S_{st}(t) = \frac{a}{k_T^{st} - k_\Delta}(e^{-k_\Delta t} - e^{-k_T^{st} t}) \tag{11}$$

where a is a constant. Respective rate constants k_Δ and k_T^{st} were found to be equal to $(2.65 \pm 0.05) \times 10^5$ s^{-1} and $(5.54 \pm 0.08) \times 10^5$ s^{-1}. The faster process has been assigned[20] to the triplet decay, the slower one to the $^1O_2$ decay. The rate constants measured by us agree well with those reported previously.[48] Subsequently, the integral intensity of luminescence emitted by photosensitized $^1O_2$, generated by the standard, can be calculated using the equation: $I_{st} = a/(k_\Delta k_T^{st})$.

3.6. A Minimal Kinetic Model. A general reaction scheme for the $^1O_2$ generation by Zn-substituted myoglobin and for a subsequent $^1O_2$ deactivation is depicted in Scheme 3. The model that we chose to present here may be considered as a minimal model because it contains the fewest number of intermediates consistent with the idea that $^1O_2$ deactivation in the protein matrix differs from that in the surrounding medium. In extra-liganded ZnPP buried inside the protein, the intersystem crossing (Scheme 3, ISC) from the singlet to triplet state has the high efficiency, ~90%. Upon photon absorption, the rapid and efficient intersystem crossing creates the lowest excited triplet state that is long-lived enough to generate singlet oxygen (Scheme 3, $k_{T\Delta}$). Obviously, there is a probability of deactivation of ZnPP triplet state by the ground state molecular oxygen without $^1O_2$ production (Scheme 3, k_{TO_2}) and a probability of triplet state deactivation in the absence of molecular oxygen (k_{T0}). The $^1O_2$ generation requires an actual short-range interaction of molecular oxygen with the photosensitizer buried deep inside the protein. Therefore, all $^1O_2$ molecules are produced within the protein matrix. Subsequently, singlet oxygen can emit light at 1270 nm

dx.doi.org/10.1021/jp501615h | J. Phys. Chem. A 2014, 118, 1864−1878

Table 4. List of Frequently Used Symbols

A_0	amplitude of light-induced triplet−triplet absorption changes at zero time
D	medium-dependent diffusion constant
f_Δ	fraction of sensitizer triplets deactivated by molecular oxygen with $^1O_2$ production
f_Δ^s	fraction of $^1O_2$ molecules escaped from the protein into the surrounding medium after photosensitization
I	integral intensity of luminescence
k_q	medium-dependent bimolecular rate constant of the triplet state quenching by molecular oxygen
k_T	rate constant for sensitizer triplet state deactivation
k_{T0}	rate constant for sensitizer triplet state deactivation in the absence of molecular oxygen
$k_{T\Delta}$	rate constant of energy transfer between the excited triplet state of sensitizer and the ground state molecular oxygen with $^1O_2$ production
k_{TO_2}	rate constant for deactivation of sensitizer triplet state by the ground state molecular oxygen without $^1O_2$ production
k_r	rate constant of medium-dependent $^1O_2$ radiative decay
k_{nr}	rate constant of medium-dependent $^1O_2$ nonradiative decay
k_a^s	rate constant for $^1O_2$ deactivation in water by surface-exposed amino acids of the protein
k_Δ	rate constant for $^1O_2$ deactivation in water
k_Δ^p	rate constant for $^1O_2$ deactivation within the protein
k'	rate constant for the bimolecular O_2 rebinding to ferrous myoglobin
k'_{entry}	rate constant for $^1O_2$ entry into Zn-substituted myoglobin
k_{escape}	rate constant for $^1O_2$ escape from Zn-substituted myoglobin
K_{entry}	equilibrium constant for $^1O_2$ entry into Zn-substituted myoglobin
n	refractive index
N	number of moles of photons striking upon a working volume V
Q_Δ	quantum yield of photosensitized $^1O_2$ generation
Q_T	quantum yield for singlet to triplet intersystem crossing, i.e., the triplet quantum yield
S	intensity of luminescence
V	working volume
$[O_2]$	concentration of molecular oxygen
$[^1O_2]$	concentration of singlet oxygen
$[^1O_2^s]$	concentration of singlet oxygen in the surrounding medium
$[^1O_2^p]$	concentration of singlet oxygen within the protein
$[^3O_2^p]$	concentration of ground state molecular oxygen within the protein
$[P]$	protein concentration
$[T_1]$	concentration of the sensitizer triplet state
α_1	rate constant for deactivation of ZnPP triplet state
α_2	rate constant for $^1O_2$ disappearance in the surrounding medium
α_3	rate constant for $^1O_2$ disappearance within the protein
β	absorption factor
γ	quantum yield of bimolecular O_2 rebinding to ferrous myoglobin
γ_0	primary quantum yield of photodissociation of molecular oxygen from ferrous myoglobin
φ	fluorescence quantum yield
φ_Δ	probability of medium-dependent radiative $^1O_2$ deactivation
κ	proportionality constant that contains geometrical and electronic factors of the detection system
τ_s	lifetime of the excited singlet state of porphyrin-related compounds
τ_T	lifetime of the excited triplet state of porphyrin-related compounds
τ_{T0}	lifetime of the excited triplet state of porphyrin-related compounds in oxygen-free mediums

(Scheme 3, k_r^p) or decay nonradiatively within the protein matrix by colliding with quenchers (k_{nr}^p): ZnPP or protein amino acids. Furthermore, singlet oxygen can escape from the protein (Scheme 3, k_{escape}). Subsequently, singlet oxygen can emit light (Scheme 3, k_r^s) or decay nonradiatively by colliding with solvent molecules (k_{nr}^s) or surface-exposed amino acids of the protein (k_a^s). Furthermore, for $^1O_2$ molecules escaped into

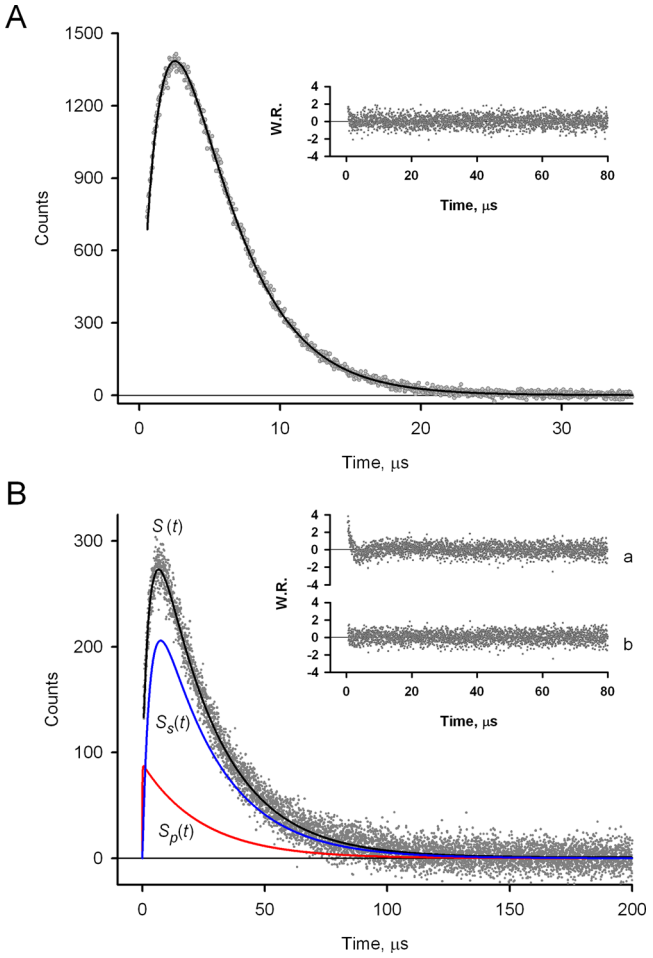

Figure 5. Time-resolved luminescence emitted by singlet oxygen photosensitized by TMPyP (A) and Zn-substituted myoglobin (B). The average noise level was subtracted from the kinetics. Concentrations of TMPyP and Zn-substituted myoglobin, 17 and 50 μM, respectively. Conditions: 50 mM citrate-phosphate buffer, pH 7.4, at 18 °C. Excitation wavelength, λ_{exc} = 532 nm; detection wavelength, λ_{det} = 1270 nm. The experimental kinetics were analyzed in the time window from 576 ns to ~350 μs, where scattered laser light and photosensitizer fluorescence do not markedly contribute to the observed data of $^1O_2$ emission. In panel A, symbols correspond to experimental data, the solid line shows data fit with eq 11, and the inset shows the weighted residuals of the fit. The weighted residuals lie within two standard deviations. In panel B, points correspond to experimental data, and the solid line designated $S(t)$ shows data fit with eq 48. Additionally, the time dependences of luminescence emitted by $^1O_2$ in the surrounding medium, $S_s(t)$, as well as in the protein, $S_p(t)$, are shown by solid blue and red lines, respectively. In panel B, insets a and b show data fit with eqs 11 and 48, respectively.

the surrounding medium, there is a probability of re-entry into the protein (Scheme 3, k'_{entry}). Values of the rate constants for $^1O_2$ escape from, k_{escape}, and entry into myoglobin, k'_{entry}, were provided by the flash photolysis experiments (see, Section 3.4). The $^1O_2$ re-entry into the protein proceeds with the first-order rate constant calculated as $k'_{entry}[^1O_2^s]$, where $[^1O_2^s]$ is the concentration of $^1O_2$ in the surrounding medium. Because the absorption of one photon by ZnPP buried inside the protein can result in the generation of only one $^1O_2$ molecule, the concentration $[^1O_2^s]$ is expected to be smaller than the concentration of ZnPP in the excited triplet state, $[T_1]$. For the experiments performed under our conditions with the pulse

dx.doi.org/10.1021/jp501615h | J. Phys. Chem. A 2014, 118, 1864−1878

Scheme 3. Reaction Scheme for $^1O_2$ Generation by Zn-Substituted Myoglobin and for Subsequent $^1O_2$ Deactivation

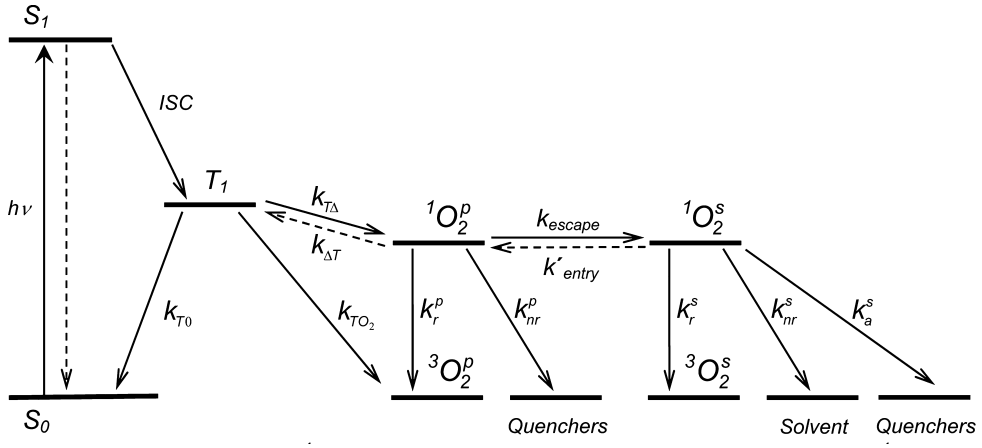

energy of 1 μJ and the excitation volume of 1.4×10^{-4} L, the concentration of T_1 states produced per laser pulse is $\sim 8 \times 10^{-9}$ M. Thus, the first-order rate constant for $^1O_2$ re-entry into the protein was estimated to be smaller than 0.3 s^{-1}. As will be shown in Section 3.7, singlet oxygen escaped from the protein is expected to be quenched by the surface-exposed amino acids with the bimolecular rate constant of $k_a^s = 4 \times 10^8$ $M^{-1}\cdot s^{-1}$, the corresponding first-order rate constant being equal to 2×10^4 s^{-1}. One can see that the first-order rate constant for $^1O_2$ re-entry into the protein is at least 4 orders of magnitude smaller than the rate constant for $^1O_2$ deactivation in water by the surface-exposed amino acids and at least 7 orders of magnitude smaller than the rate constant for $^1O_2$ escape from the protein, k_{escape} (Table 3). Therefore, the $^1O_2$ re-entry into the protein can be neglected under the conditions employed. Moreover, the energy back transfer from singlet oxygen to the ground state photosensitizer (Scheme 3, $k_{\Delta T}$) can also be neglected. In the case of a considerable rate constant for the energy back transfer, $k_{\Delta T}$, the kinetics of the triplet−triplet absorption of Zn-substituted myoglobin would be described by a more complicated function than the single exponential function observed in the present flash photolysis experiments (see the Triplet−Triplet Absorption subsection in Section 3.2).

It should be noted that the local concentration of ground state molecular oxygen inside the protein differs from that in water. This internal concentration does not appear to be definable in any simple way since it is likely to vary from one region of the protein to another.[50] We assumed that, at least to a first approximation, ground state molecular oxygen is present in the protein matrix before laser irradiation at an equilibrium concentration, denoted hereafter as $[^3O_2^p]$. Moreover, we assumed that the laser energy is low enough to not markedly change the equilibrium concentration of molecular oxygen within the protein matrix as well as in the aqueous phase. Hence, the equilibrium concentration of ground state molecular oxygen within the protein matrix was considered to be constant and equal to $[^3O_2^p]$ during the measurements. Additionally, the protein concentration, [P], was considered to be constant in a working volume at the constant magnetic stirring of the solutions.

According to Scheme 3, the system of coupled differential equations providing the time dependence of the concentration of ZnPP triplet state, $[T_1](t)$, the concentration of $^1O_2$ within the protein, $[^1O_2^p](t)$, as well as in the surrounding medium, $[^1O_2^s](t)$, may be set as

$$\frac{d[T_1](t)}{dt} = -k_{T0}[T_1](t) - (k_{T\Delta} + k_{TO_2})[^3O_2^p][T_1](t) \quad (12)$$

$$\frac{d[^1O_2^p](t)}{dt} = -(k_r^p + k_{nr}^p + k_{escape})[^1O_2^p](t) + k_{T\Delta}[^3O_2^p][T_1](t) \quad (13)$$

$$\frac{d[^1O_2^s](t)}{dt} = -(k_r^s + k_{nr}^s + k_a^s[P])[^1O_2^s](t) + k_{escape}[^1O_2^p](t) \quad (14)$$

where k_{T0} is the first-order rate constant for deactivation of ZnPP triplet state in the absence of molecular oxygen; k_{TO_2} is the bimolecular rate constant for deactivation of ZnPP triplet state by the ground state molecular oxygen without $^1O_2$ production; $k_{T\Delta}$ is the bimolecular rate constant of energy transfer between the ZnPP triplet state and the ground state molecular oxygen with $^1O_2$ production; k_r and k_{nr} are the medium-dependent $^1O_2$ radiative and nonradiative rate constants, respectively; k_a^s is the bimolecular rate constant for $^1O_2$ deactivation in water by the surface-exposed amino acids of the protein.

In eqs 13 and 14, the sum of the medium-dependent $^1O_2$ radiative, k_r, and nonradiative rate constants, k_{nr}, determines the rate constant for $^1O_2$ deactivation within the protein, k_Δ^p, and in water, k_Δ, respectively:

$$k_\Delta^p = k_r^p + k_{nr}^p \quad (15)$$

$$k_\Delta = k_r^s + k_{nr}^s \quad (16)$$

To solve the system of eqs 12−14, the initial concentration of T_1-state was set equal to $[T_1]_{t=0}$, while that of $^1O_2$ within the protein and in the surrounding medium were set to zero. Thus, solving the system of differential equations, one can obtain the time dependence of the concentration of T_1-state:

$$[T_1](t) = [T_1]_{t=0}e^{-\alpha_1 t} \quad (17)$$

the concentration of $^1O_2$ within the protein:

$$[^1O_2^p](t) = \frac{k_{T\Delta}[^3O_2^p][T_1]_{t=0}}{\alpha_3 - \alpha_1}(e^{-\alpha_1 t} - e^{-\alpha_3 t}) \quad (18)$$

as well as in the surrounding medium:

dx.doi.org/10.1021/jp501615h | J. Phys. Chem. A 2014, 118, 1864−1878

$$[^1O_2^s](t) = \frac{k_{escape}k_{T\Delta}[^3O_2^p][T_1]_{t=0}}{(\alpha_3-\alpha_2)(\alpha_3-\alpha_1)(\alpha_2-\alpha_1)} ((\alpha_3-\alpha_2)e^{-\alpha_1 t} - (\alpha_3-\alpha_1)e^{-\alpha_2 t} + (\alpha_2-\alpha_1)e^{-\alpha_3 t}) \quad (19)$$

Here,

$$\alpha_1 = k_T = k_{T0} + (k_{T\Delta} + k_{TO_2})[^3O_2^p] \quad (20)$$

$$\alpha_2 = k_\Delta + k_a^s[P] \quad (21)$$

$$\alpha_3 = k_\Delta^p + k_{escape} \quad (22)$$

As it is followed from eqs 20−22, α_1 is the rate constant for deactivation of ZnPP triplet state; α_2 and α_3 are the rate constants for $^1O_2$ disappearance in the surrounding medium and within the protein matrix, respectively. Using eqs 21 and 22, the bimolecular rate constant for $^1O_2$ deactivation in water by the surface-exposed amino acids of the protein, k_a^s, and the rate constant for $^1O_2$ deactivation within the protein, k_Δ^p, can be expressed through the experimentally measured parameters

$$k_a^s = (\alpha_2 - k_\Delta)/[P] \quad (23)$$

$$k_\Delta^p = \alpha_3 - k_{escape} \quad (24)$$

Luminescence Emitted by $^1O_2$ Photosensitized by Zn-Substituted Myoglobin. The intensity of luminescence emitted by $^1O_2$ photosensitized by Zn-substituted myoglobin, $S(t)$, is equal to the sum of the intensity of luminescence emitted by $^1O_2$ in the protein, $S_p(t)$, and in the surrounding medium, $S_s(t)$:

$$S(t) = S_p(t) + S_s(t) \quad (25)$$

The intensities $S_p(t)$ and $S_s(t)$ are proportional to the concentrations of $^1O_2$ within the protein, $[^1O_2^p](t)$, and in the surrounding medium, $[^1O_2^s](t)$, respectively:

$$S_p(t) = \frac{\kappa}{n^2}k_r^p[^1O_2^p](t) \quad (26)$$

$$S_s(t) = \frac{\kappa}{n^2}k_r^s[^1O_2^s](t) \quad (27)$$

Taking into account eqs 18 and 19, one can obtain the time dependence of luminescence emitted by $^1O_2$ photosensitized by Zn-substituted myoglobin in terms of the experimentally measured parameters, $\chi_i (i = 1,2)$ and α_i ($i = \overline{1, 3}$):

$$S(t) = \chi_1 e^{-\alpha_1 t} - \chi_2 e^{-\alpha_2 t} + (\chi_2 - \chi_1)e^{-\alpha_3 t} \quad (28)$$

where

$$\chi_1 = \frac{\kappa\, k_r^s[T_1]_{t=0}}{n^2}\frac{\left(k_{escape} + \xi(\alpha_2-\alpha_1)\right)k_{T\Delta}[^3O_2^p]}{(\alpha_2-\alpha_1)(\alpha_3-\alpha_1)} \quad (29)$$

$$\chi_2 = \frac{\kappa k_r^s[T_1]_{t=0}}{n^2}\frac{k_{escape}k_{T\Delta}[^3O_2^p]}{(\alpha_2-\alpha_1)(\alpha_3-\alpha_2)} \quad (30)$$

$$\xi = k_r^p/k_r^s \quad (31)$$

Moreover, in terms of the experimentally determined parameters, the time dependence of luminescence emitted by $^1O_2$ in the protein, $S_p(t)$, can be expressed using eqs 26, 18, 29, and 30:

$$S_p(t) = \left(\chi_1 - \chi_2\frac{\alpha_3-\alpha_2}{\alpha_3-\alpha_1}\right)(e^{-\alpha_1 t} - e^{-\alpha_3 t}) \quad (32)$$

Similarly, taking into account eqs 27, 19, and 30, the time dependence of luminescence emitted by $^1O_2$ in the surrounding medium, $S_s(t)$, can be obtained:

$$S_s(t) = \frac{\chi_2}{\alpha_3-\alpha_1}((\alpha_3-\alpha_2)e^{-\alpha_1 t} - (\alpha_3-\alpha_1)e^{-\alpha_2 t} + (\alpha_2-\alpha_1)e^{-\alpha_3 t}) \quad (33)$$

In their turn, upon integrating eqs 28, 32, and 33 with respect to the time, one can express the total detected integral intensity of luminescence emitted by $^1O_2$ photosensitized by Zn-substituted myoglobin, I, as well as the integral intensity of luminescence emitted by $^1O_2$ in the protein, I_p, and in the surrounding medium, I_s, respectively:

$$I = \frac{\chi_1}{\alpha_1} - \frac{\chi_2}{\alpha_2} + \frac{\chi_2 - \chi_1}{\alpha_3} \quad (34)$$

$$I_p = \frac{\chi_1(\alpha_3-\alpha_1) - \chi_2(\alpha_3-\alpha_2)}{\alpha_1\alpha_3} \quad (35)$$

$$I_s = \frac{\chi_2}{\alpha_3-\alpha_1}\left(\frac{\alpha_3-\alpha_2}{\alpha_1} - \frac{\alpha_3-\alpha_1}{\alpha_2} + \frac{\alpha_2-\alpha_1}{\alpha_3}\right) \quad (36)$$

Quantum Yield of $^1O_2$ Generation by Zn-Substituted Myoglobin. The number of $^1O_2$ molecules formed per absorbed photon by a sensitizer defines the quantum yield of photosensitized $^1O_2$ generation, Q_Δ. The quantum yield of $^1O_2$ generation by the chosen standard, Q_Δ^{st}, is known to be equal to 0.77 ± 0.04.[48] The quantum yield Q_Δ is determined by two factors:

$$Q_\Delta = Q_T f_\Delta \quad (37)$$

Here, Q_T is the triplet quantum yield, defined as the amount of sensitizers in the photoexcited triplet state relative to the amount of originally excited chromophores:

$$Q_T = \frac{[T_1]_{t=0}}{(N/V)\beta} \quad (38)$$

where N is the number of moles of photons striking upon a working volume V. β is the sensitizer absorption factor determined by $\beta = 1 - 10^{-A}$, where A is the sensitizer absorbance at the excitation wavelength. The second factor in eq 37, f_Δ, is the fraction of triplets deactivated by molecular oxygen with $^1O_2$ production. The factors f_Δ for the standard and for Zn-substituted myoglobin are given by

$$f_\Delta^{st} = \frac{k_{T\Delta}^{st}[O_2]}{k_T^{st}} \quad (39)$$

$$f_\Delta = \frac{k_{T\Delta}[^3O_2^p]}{\alpha_1} \quad (40)$$

respectively.

The detected integral intensity of luminescence emitted by $^1O_2$ photosensitized by the standard, I_{st}, can be expressed in terms of the quantum yield of $^1O_2$ generation, Q_Δ^{st}, using eqs 10, 37, 38, and 39:

dx.doi.org/10.1021/jp501615h | J. Phys. Chem. A 2014, 118, 1864−1878

Table 5. Parameters Describing the Emission and Deactivation of Singlet Oxygen Generated by Zn-Substituted Myoglobin

pH	α_1 (ms^{-1})	α_2 (ms^{-1})	α_3 (μs^{-1})	k_a^s ($nM^{-1}\cdot s^{-1}$)	k_Δ^p, k_{nr}^p (μs^{-1})	k_r^p (s^{-1})	$\xi = k_r^p/k_r^s$	I_p/I	Q_Δ	f_Δ^s
7.4	41 ± 1	315 ± 10	10.8 ± 1.3	0.9 ± 0.5	4.3 ± 1.3	1.6 ± 0.4	7.5 ± 1.7	0.26 ± 0.03	0.9 ± 0.1	0.60 ± 0.09
4.9	42 ± 1	300 ± 10	11.3 ± 1.7	0.7 ± 0.5	4.4 ± 1.8	1.8 ± 0.4	8.7 ± 2.1	0.27 ± 0.06	0.9 ± 0.1	0.62 ± 0.11
average[a]: 4.9–7.4						1.7 ± 0.3	8.1 ± 1.3			

Concentration of Zn-substituted myoglobin is 50 μM. Conditions: 50 mM citrate-phosphate buffer, at 18 °C. The uncertainties are presented as 95% confidence intervals. In the present work, for the directly measured parameters including α_1 and α_2, the mean values and uncertainties were obtained from independently repeated experiments. Subsequently, for any other parameter, the mean value and uncertainty were calculated as $F(\langle p_1\rangle,...,\langle p_m\rangle)$ and $(\sum_{j=1}^{m}((\partial F)/(\partial p_j))^2\Delta p_j^2)^{1/2}$, respectively. Here, F is a function of m determined parameters, p_j ($j = \overline{1, m}$); $\langle p_j\rangle$ and Δp_j are the mean value and uncertainty for the parameter p_j, respectively; the partial derivatives are evaluated at the mean values of the parameters. [a]The mean value of ξ, $\langle\xi\rangle$, and its 95% confidence interval, $\Delta\xi$, were calculated as: $\langle\xi\rangle = (1/n)\sum_{i=1}^{n}\xi_i$ and $\Delta\xi = (1/n)\cdot(\sum_{i=1}^{n}\Delta\xi_i^2)^{1/2}$, respectively; $n = 2$.

$$I_{st} = \frac{\kappa}{n^2}Q_\Delta^{st}\frac{k_r^s}{k_\Delta}\left(\frac{N}{V}\right)\beta_{st} \tag{41}$$

Similarly, the detected integral intensity of luminescence emitted by $^1O_2$ in the protein, I_p, and in the surrounding medium, I_s, after the photosensitized generation by Zn-substituted myoglobin can be written, respectively, as

$$I_p = \frac{\kappa}{n^2}Q_\Delta\varphi_\Delta^p(N/V)\beta \tag{42}$$

$$I_s = \frac{\kappa}{n^2}Q_\Delta f_\Delta^s\varphi_\Delta^s(N/V)\beta \tag{43}$$

where φ_Δ^p and φ_Δ^s are the probabilities of radiative $^1O_2$ deactivation within the protein and in the surrounding medium, respectively:

$$\varphi_\Delta^p = k_r^p/\alpha_3 \tag{44}$$

$$\varphi_\Delta^s = k_r^s/\alpha_2 \tag{45}$$

f_Δ^s is the fraction of $^1O_2$ molecules escaped from the protein into the surrounding medium after photosensitization:

$$f_\Delta^s = k_{escape}/\alpha_3 \tag{46}$$

Finally, dividing eq 43 by eq 41 and taking into account eqs 45 and 46, the quantum yield of $^1O_2$ generation by Zn-substituted myoglobin can be expressed in terms of the experimentally measured parameters:

$$Q_\Delta = Q_\Delta^{st}\frac{I_s}{I_{st}}\frac{\alpha_2\alpha_3}{k_{escape}k_\Delta}\frac{\beta_{st}}{\beta} \tag{47}$$

3.7. Deactivation of $^1O_2$ Photosensitized by Zn-Substituted Myoglobin. Typical time-resolved trace of luminescence emitted at 1270 nm by $^1O_2$ photosensitized by Zn-substituted myoglobin is shown in Figure 5B. Careful spectral analysis proved that scattered laser light and photosensitizer fluorescence disappear almost completely during the first 576 ns after the photoexcitation (not shown). In a specially chosen time window from 576 ns to ~350 μs, where the scattered laser light and photosensitizer fluorescence do not markedly contribute to the observed data of $^1O_2$ emission, the $^1O_2$ signal was analyzed. The chosen time interval is appropriate for measurements of the rate constant for deactivation of ZnPP triplet state, α_1, and the rate constant for $^1O_2$ disappearance in the surrounding medium, α_2, while it is not suitable for measurements of the rate constant for $^1O_2$ disappearance within the protein matrix, α_3. According to eq 22, the rate constant α_3 is determined by the sum of the rate constant for $^1O_2$ deactivation within the protein, k_Δ^p, and the rate constant for $^1O_2$ escape from Zn-substituted myoglobin, k_{escape}. Taking the measured value of k_{escape} (Table 3) as the lower limit for the rate constant α_3, one can obtain that singlet oxygen disappears within the protein matrix in less than ~150 ns after photosensitization, i.e., too fast to be detected in the chosen time window. Consequently, under the chosen experimental conditions, the third term in eq 28 can be neglected. Therefore, it is expected that the time dependence of the observed $^1O_2$ luminescence is characterized by the equation

$$S(t) = \chi_1 e^{-\alpha_1 t} - \chi_2 e^{-\alpha_2 t} \tag{48}$$

The rate constants α_1 and α_2, found by fitting the observed kinetics to eq 48, are listed in Table 5. The values of the rate constant for deactivation of ZnPP triplet state, α_1 (Table 5), determined in the present $^1O_2$ emission study, are the same as those measured by the flash photolysis technique, k_T (Triplet–Triplet Absorption subsection in Section 3.2). As it is seen from Figure 5B, the observed kinetics (dots) fit well to eq 48 (black line). Weighted residuals from the fit are randomly distributed around zero (Figure 5B, inset b) and lie within two standard deviations. It is necessary to stress that the observed kinetics is not adequately described by eq 11, applied in the case of a homogeneous environment. Weighted residuals from the corresponding fit are nonrandomly distributed around zero (Figure 5B, inset a). These findings unequivocally demonstrate that the samples of Zn-substituted myoglobin are spatially nonhomogeneous for $^1O_2$ emission.

The rate constant for $^1O_2$ disappearance within the protein matrix, α_3, though not detected by the direct measurements, can be evaluated by taking into account parameters that describe luminescence emitted by $^1O_2$ generated by the standard. Assuming that $k_{T\Delta} \gg k_{TO_2}$ [39] and modifying eqs 30, 38, and 41, the rate constant α_3 can be expressed in terms of the experimentally determined parameters

$$\alpha_3 = \alpha_2 + I_{st}\frac{Q_T}{Q_\Delta^{st}}\frac{k_{escape}k_\Delta\alpha_1}{\chi_2(\alpha_2 - \alpha_1)}\frac{\beta}{\beta_{st}} \tag{49}$$

α_3 values obtained at pH 7.4 and 4.9 are listed in Table 5. Putting the found empirical parameters α_i ($i = \overline{1, 3}$) and χ_i (i = 1,2) into eqs 32 and 33, the time dependences of luminescence emitted by $^1O_2$ in the protein, $S_p(t)$, as well as in the surrounding medium, $S_s(t)$, were obtained and shown in Figure 5 by red and blue lines, respectively. Subsequently, using eqs 34–36, the integral intensity of luminescence emitted by $^1O_2$ in the protein, I_p, and in the surrounding medium, I_s, as well as the contribution of the integral intensity of luminescence emitted by $^1O_2$ in the protein to the total integral intensity, I_p/I, were calculated. The last one is equal to ~0.26 (Table 5). Moreover,

dx.doi.org/10.1021/jp501615h | J. Phys. Chem. A 2014, 118, 1864–1878

using eq 47, the quantum yield of $^1O_2$ generation by Zn-substituted myoglobin, Q_Δ, was calculated (Table 5). As it is seen, the quantum yield of $^1O_2$ generation, $Q_\Delta = 0.9 \pm 0.1$ (Table 5), is equal to the triplet quantum yield of Zn-substituted myoglobin, $Q_T = 0.90 \pm 0.05$ (see Triplet Quantum Yield in Section 3.2). Therefore, every collision of ground state molecular oxygen with ZnPP in the excited triplet state results in $^1O_2$ generation within the protein matrix. We may thus state with confidence that, for Zn-substituted myoglobin, the bimolecular rate constant for ZnPP triplet state quenching by molecular oxygen, k_q^p (Triplet−Triplet Absorption in Section 3.2), is smaller compared with that for monomeric ZnPP in the aqueous solutions, k_q^s, due to a decrease in the number of collisions between molecular oxygen and the porphyrin and not due to a change in the overall efficiency of ZnPP triplet state deactivation.

Nonradiative $^1O_2$ Deactivation in Water by Surface-Exposed Amino Acids of the Protein. After photosensitization, some $^1O_2$ molecules escape from the protein. The fraction of $^1O_2$ molecules escaped into the surrounding medium after photosensitization, f_Δ^s, determined with the use of eq 46, is equal to ~0.6 (Table 5). On the average, six from every 10 $^1O_2$ molecules succeed in escaping from the protein matrix. Subsequently, singlet oxygen can emit light or decay nonradiatively by colliding with solvent molecules or surface-exposed amino acids of the protein. The bimolecular rate constant for $^1O_2$ deactivation in water by surface-exposed amino-acids of the protein, k_a^s, was calculated using eq 23 and listed in Table 5. Quenching of singlet oxygen escaped from the protein, to a first approximation, depends on the presence of reactive solvent-exposed amino acids in the protein and on the accessibility of these amino acids to singlet oxygen. The aromatic amino acids tyrosine and tryptophan as well as histidine and the sulfur-containing methionine and cysteine are primary sites of attack by singlet oxygen, while the aliphatic amino acids and peptide bonds react with a significantly lower rate.[51] In horse heart myoglobin, there are 11 histidine, 2 tryptophan, 2 methionine, and 2 tyrosine residues. The bimolecular rate constant for $^1O_2$ quenching with the corresponding free, solvated amino acids is known to be equal to 6×10^7 $M^{-1}\cdot s^{-1}$,[52] 6×10^7 $M^{-1}\cdot s^{-1}$,[52] ~1.5×10^7 $M^{-1}\cdot s^{-1}$,[52] and ~0.5×10^7 $M^{-1}\cdot s^{-1}$,[51] respectively. Moreover, there are 15 alanine and 7 phenylalanine residues that are expected to exhibit the least ability to quench singlet oxygen. The bimolecular rate constant for $^1O_2$ quenching with solvated alanine and phenylalanine are equal to ~1×10^6 $M^{-1}\cdot s^{-1}$ and ~7×10^5 $M^{-1}\cdot s^{-1}$,[53,51] respectively. X-ray crystal structure analysis of horse heart myoglobin (PDB code 1AZI) showed that some of the amino acids are exposed on the protein surface, while some amino acids are buried in the protein interior. Obviously, the buried amino acids contribute less or nothing to $^1O_2$ quenching in water. On the other hand, the behavior of the surface-exposed amino acids is not expected to differ appreciably from that of the isolated amino acids. The surface-exposed amino acids were found to be His36, 48, 81, 113, 116, 119, and Tyr103. Moreover, there are also nine alanine and one phenylalanine surface-exposed residues. Implying that the surface-exposed amino acids are all about equally accessible to singlet oxygen, the bimolecular rate constant for $^1O_2$ deactivation by these amino acids, k_a^s, can be approximated by the sum of the bimolecular rate constants for $^1O_2$ quenching by the corresponding free, solvated amino acids.[51−53] The rate constant k_a^s thus estimated has a value of 0.4×10^9 $M^{-1}\cdot s^{-1}$, which is consistent with the experimentally measured values of k_a^s (Table 5).

Nonradiative $^1O_2$ Deactivation within the Protein. After photosensitization, singlet oxygen can decay nonradiatively within the protein matrix by colliding with ZnPP or protein amino acids. According to eq 24, the value of the rate constant for $^1O_2$ deactivation within the protein, k_Δ^p, differs from that of the rate constant for $^1O_2$ disappearance within the protein matrix, α_3 (Table 5), by the value of the rate constant for $^1O_2$ escape from the protein, k_{escape} (Table 3). The rate constant k_Δ^p was calculated and listed in Table 5. In their turn, according to eq 15, the rate constant k_Δ^p is determined by the sum of the protein-dependent $^1O_2$ radiative, k_r^p, and nonradiative rate constants, k_{nr}^p. As will be shown later, the radiative rate constant k_r^p is six orders in magnitude smaller than the rate constant k_Δ^p, indicating that the value of k_Δ^p is determined mainly by the value of the nonradiative rate constant, k_{nr}^p. Hence, k_{nr}^p is considered to be equal to k_Δ^p (Table 5). It is known that the radiative as well as nonradiative $^1O_2$ deactivation is a bimolecular process in the gas and condensed phases. Collisions of singlet oxygen with each protein amino acid and the photosensitizer are expected to contribute independently to the overall probability of $^1O_2$ deactivation within the protein. Each contribution is given by the product of the individual quencher concentration and the bimolecular rate constant for $^1O_2$ deactivation by the quencher. Obviously, in the protein matrix, the bimolecular rate constant for $^1O_2$ deactivation by an individual quencher is directly proportional to the diffusion constant for singlet oxygen. Assuming that singlet oxygen is deactivated by an individual quencher in the protein with efficiency equal to that in the solvent, the expected rate constant k_Δ^p can be obtained by the following equation:

$$k_\Delta^p = (D_p/D_s) \sum_i k_\Delta^i [Q_i] \tag{50}$$

where k_Δ^i is the bimolecular rate constant for $^1O_2$ deactivation by the ith quencher, the rate constant being determined mainly by nonradiative $^1O_2$ deactivation. Obviously, the values of k_Δ^i in eq 50 are taken for free, solvated quenchers. In particular, the bimolecular rate constant for $^1O_2$ deactivation by solvated ZnPP was taken to be 2×10^7 M^{-1} s^{-1}.[54] The rate constants for $^1O_2$ deactivation by solvated amino acids were mentioned above. In eq 50, $[Q_i]$ is the concentration of the ith quencher in the protein. The molarities of the quenchers in the protein were calculated by utilizing the protein volume. The difference in the diffusion constants for singlet oxygen in the aqueous solutions, D_s, and in the protein, D_p, was taken into account. The diffusion constant in the protein, D_p, was taken to be in 8.6 ± 0.3 times smaller than that in the aqueous solutions, D_s (see Triplet−Triplet Absorption in Section 3.2). Thus, the expected rate constant for $^1O_2$ deactivation within the protein, k_Δ^p, was calculated to be $(4.8 \pm 0.2) \times 10^6$ s^{-1}, which is in excellent agreement with the values of $(4.3 \pm 1.3) \times 10^6$ s^{-1} and $(4.4 \pm 1.8) \times 10^6$ s^{-1}, found experimentally at pH 7.4 and 4.9, respectively (Table 5). Therefore, the nonradiative $^1O_2$ deactivation process within the protein can be expressed as the sum of the independent processes of $^1O_2$ quenching by each individual amino acid and the photosensitizer, the efficiency of $^1O_2$ deactivation by a given individual quencher in the protein being equal to that in the aqueous solutions.

Radiative $^1O_2$ Deactivation within the Protein. After photosensitization, singlet oxygen can emit light from the protein matrix. The ratio between the first-order radiative rate

constant for $^1O_2$ deactivation within the protein, k_r^p, and the one in the surrounding medium, k_r^s, can be expressed in terms of the experimentally measured parameters dividing eq 42 by eq 43 and taking into account eqs 44−46:

$$\xi = \frac{k_r^p}{k_r^s} = \frac{I_p}{I_s}\frac{k_{escape}}{\alpha_2} \quad (51)$$

The found values of ξ are listed in Table 5. Additionally, the mean value of ξ obtained at pH 7.4 and 4.9 was calculated. The mean value of ξ is equal to 8.1 ± 1.3 (Table 5). The present result indicates the strong influence of the protein matrix on the radiative $^1O_2$ deactivation. Taking the first-order radiative rate constant for $^1O_2$ deactivation in water to be equal to $k_r^s = 0.209$ s^{-1},[55] one can obtain the first-order radiative rate constant for $^1O_2$ deactivation within the protein: $k_r^p = k_r^s \xi$. The data are listed in Table 5. The mean first-order radiative rate constant k_r^p was found to be equal to 1.7 ± 0.3 s^{-1}. It should be noted that effects of solvent on the first-order radiative rate constant k_r have been the subject of intense experimental investigations.[56−59] A correlation of the first-order radiative rate constant k_r with the solvent refractive index n has been observed in pure solvents (see, for example, ref 57). According to the correlation,[57] in pure solvents with the bulk refractive index n = 1.6, as in the case of the studied protein,[60] the first-order radiative rate constant, k_r, is expected to be equal to 1.6 s^{-1}. As is seen, there is a good agreement between the experimentally determined radiative rate constant for $^1O_2$ deactivation within myoglobin, k_r^p, and that for $^1O_2$ deactivation in the pure solvents, k_r. We concluded that the determined radiative rate constant k_r^p is reasonable. Although the protein is hardly a homogeneous medium, the unique values of k_r^p and k_{nr}^p can represent an average radiative and nonradiative $^1O_2$ deactivation within the protein matrix.

Like the nonradiative $^1O_2$ deactivation within the protein, the radiative $^1O_2$ deactivation can be considered as a bimolecular process. Collisions of singlet oxygen with each protein amino acid and the photosensitizer can be assumed to contribute independently to the observed first-order radiative rate constant k_r^p. Each contribution is given by the product of the individual collision partner concentration and the bimolecular rate constant for radiative $^1O_2$ deactivation by the collision partner. As in the case of the gas and condensed phases, the bimolecular rate constant of the collision-induced $^1\Delta_g \rightarrow {}^3\Sigma_g^-$ emission in the protein matrix is expected to depend on molecular parameters such as collision frequency, molecular size, and molecular polarizability of the individual collision partner.[1,55,58] On the other hand, the authors of ref 61 demonstrated that the radiative rate constant for $^1O_2$ deactivation responds to an ensemble of interacting solvent molecules rather than the individual collision partner. Therefore, it is now particularly interesting to examine the radiative as well as nonradiative $^1O_2$ deactivation within proteins that have other amino acid compositions.

4. CONCLUSIONS

In the present work, the nanosecond laser near-infrared spectrometer was used to study $^1O_2$ emission in a protein matrix. Myoglobin in which the intact heme is substituted by ZnPP was employed. Every collision of ground state molecular oxygen with ZnPP in the excited triplet state results in $^1O_2$ generation within the protein matrix. The quantum yield of $^1O_2$ generation by Zn-substituted myoglobin was found to be equal to 0.9 ± 0.1. On the average, six from every 10 $^1O_2$ molecules succeed in escaping from the protein matrix into the solvent. Therefore, Zn-substituted myoglobin is an efficient singlet oxygen photosensitizer in bulk water. For Zn-substituted myoglobin, the bimolecular rate constant for ZnPP triplet state quenching by molecular oxygen is smaller compared with that for monomeric ZnPP in the aqueous solutions due to a decrease in the number of collisions between molecular oxygen and the porphyrin and not due to a change in the overall efficiency of ZnPP triplet state deactivation.

The kinetic model for $^1O_2$ generation within the protein matrix and for the subsequent $^1O_2$ deactivation was introduced and discussed. To our knowledge, this is the first model that incorporates the major features of $^1O_2$ deactivation in a protein solution, including different radiative as well as nonradiative rate constants for $^1O_2$ deactivation within the protein matrix and in the surrounding medium. Using the photosensitizer buried deep inside the protein, we determined for the first time the rate constants for radiative as well as nonradiative $^1O_2$ deactivation within the protein matrix. The consistency of the experimentally measured rate constants with those predicted based on the literature data is remarkable. It was found that the nonradiative $^1O_2$ deactivation process within the protein can be expressed as the sum of the independent processes of $^1O_2$ quenching by each individual amino acid and the photosensitizer, the efficiency of $^1O_2$ deactivation by a given individual quencher in the protein being equal to that in the aqueous solutions. The first-order radiative rate constant for $^1O_2$ deactivation within the protein was found to be 8.1 ± 1.3 times larger than the one in the aqueous solutions, indicating the strong influence of the protein matrix on the radiative $^1O_2$ deactivation. Collisions of singlet oxygen with each protein amino acid and the photosensitizer were assumed to contribute independently to the observed first-order radiative rate constant. Each contribution is given by the product of the individual collision partner concentration and the bimolecular rate constant for radiative $^1O_2$ deactivation by the collision partner. As in the case of the gas and condensed phases, the bimolecular rate constant of the collision-induced $^1\Delta_g \rightarrow {}^3\Sigma_g^-$ emission in the protein matrix is expected to depend on molecular parameters such as collision frequency, molecular size, and molecular polarizability of the individual collision partner.

■ ASSOCIATED CONTENT

Supporting Information

A figure showing the amplitude of the light-induced triplet−triplet absorption changes, A_0, and the triplet state lifetime of Zn-substituted myoglobin, τ_T, versus number of pump laser pulses at a constant probe illumination in multiple flash photolysis experiment. A procedure for obtaining the relationships between the empirical kinetic parameters of the geminate components and the rate constants for O_2 intraprotein rebinding, escape from within the primary docking site into the environmental medium, and movement through the protein. This material is available free of charge via the Internet at http://pubs.acs.org.

■ AUTHOR INFORMATION

Corresponding Author

*Corresponding author. Tel.: +375 17 284 0795; fax: +375 17 284 0879. E-mail: lepeshkevich@imaph.bas-net.by.

Notes

The authors declare no competing financial interest.

■ ACKNOWLEDGMENTS

The authors are greatly indebted to A.V. Yantsevich and V.A. Galievsky for fruitful discussion. The authors are grateful to V. N. Knyukshto and A. P. Stupak for their excellent technical assistance with steady-state and time-resolved fluorescence measurements, respectively. This work was supported by the Foundation of Basic Research of the Republic of Belarus (Grants No. Ph11Y-084, Ph13-016) and by the National Academy of Sciences of Belarus through the Program "Electronics and Photonics" (Project 2.3.03).

■ REFERENCES

(1) Schweitzer, C.; Schmidt, R. Physical Mechanisms of Generation and Deactivation of Singlet Oxygen. *Chem. Rev.* **2003**, *103*, 1685−1757.

(2) Minaev, B. F. Electronic Mechanisms of Molecular Oxygen Activation. *Russ. Chem. Rev.* **2007**, *76*, 988−1010.

(3) Krasnovsky, A. A., Jr. Luminescence and Photochemical Studies of Singlet Oxygen Photonics. *J. Photochem. Photobiol. A: Chem.* **2008**, *196*, 210−218.

(4) Jensen, R. L.; Arnbjerg, J.; Ogilby, P. R. Reaction of Singlet Oxygen with Tryptophan in Proteins: A Pronounced Effect of the Local Environment on the Reaction Rate. *J. Am. Chem. Soc.* **2012**, *134*, 9820−9826.

(5) Pimenta, F. M.; Jensen, R. L.; Breitenbach, T.; Etzerodt, M.; Ogilby, P. R. Oxygen-Dependent Photochemistry and Photophysics of "MiniSOG," a Protein-Encased Flavin. *Photochem. Photobiol.* **2013**, *89*, 1116−1126.

(6) Ruiz-González, R.; Cortajarena, A. L.; Mejias, S. H.; Agut, M.; Nonell, S.; Flors, C. Singlet Oxygen Generation by the Genetically-Encoded Tag MiniSOG. *J. Am. Chem. Soc.* **2013**, *135*, 9564−9567.

(7) Comas-Barceló, J.; Rodríguez-Amigo, B.; Abbruzzetti, S.; Rey-Puech, P.; Agut, M.; Nonell, S.; Viappiani, C. A Self-Assembled Nanostructured Material with Photosensitising Properties. *RSC Adv.* **2013**, *3*, 17874−17879.

(8) Kendrew, J. C.; Bodo, G.; Dintzis, H. M.; Parrish, R. G.; Wyckoff, H.; Phillips, D. C. A Three-Dimensional Model of the Myoglobin Molecule Obtained by X-ray Analysis. *Nature* **1958**, *181*, 662−666.

(9) Chatfield, M. D.; Walda, K. N.; Magde, D. Activation Parameters for Ligand Escape from Myoglobin Proteins at Room Temperature. *J. Am. Chem. Soc.* **1990**, *112*, 4680−4687.

(10) Steinbach, P. J.; Ansari, A.; Berendzen, J.; Braunstein, D.; Chu, K.; Cowen, B. R.; Ehrenstein, D.; Frauenfelder, H.; Johnson, J. B.; Lamb, D. C.; et al. Ligand Binding to Heme Proteins: Connection between Dynamics and Function. *Biochemistry* **1991**, *30*, 3988−4001.

(11) Scott, E. E.; Gibson, Q. H.; Olson, J. S. Mapping the Pathways for O_2 Entry into and Exit from Myoglobin. *J. Biol. Chem.* **2001**, *276*, 5177−5188.

(12) Lamb, D. S.; Nienhaus, K.; Arcovito, A.; Draghi, F.; Miele, A. E.; Brunori, M.; Nienhaus, G. U. Structural Dynamics of Myoglobin. Ligand Migration among Protein Cavities Studied by Fourier Transform Infrared/Temperature Derivative Spectroscopy. *J. Biol. Chem.* **2002**, *277*, 11636−11644.

(13) Tilton, R. F., Jr.; Kuntz, I. D., Jr.; Petsko, G. A. Cavities in Proteins: Structure of a Metmyoglobin − Xenon Complex Solved to 1.9 Å. *Biochemistry* **1984**, *23*, 2849−2857.

(14) Cohen, J.; Arkhipov, A.; Braun, R.; Schulten, K. Imaging the Migration Pathways for O_2, CO, NO, and Xe inside Myoglobin. *Biophys. J.* **2006**, *91*, 1844−1857.

(15) Anselmi, M.; Di Nola, A.; Amadei, A. The Kinetics of Ligand Migration in Crystallized Myoglobin as Revealed by Molecular Dynamics Simulation. *Biophys. J.* **2008**, *94*, 4277−4281.

(16) Schotte, F.; Lim, M.; Jackson, T. A.; Smirnov, A. V.; Soman, J.; Olson, J. S.; Phillips, G. N., Jr.; Wulff, M.; Anfinrud, P. A. Watching a Protein as it Functions with 150-ps Time-Resolved X-ray Crystallography. *Science* **2003**, *300*, 1944−1947.

(17) Bourgeois, D.; Vallone, B.; Schotte, F.; Arcovito, A.; Miele, A. E.; Sciara, G.; Wulff, M.; Anfinrud, P.; Brunori, M. Complex Landscape of Protein Structural Dynamics Unveiled by Nanosecond Laue Crystallography. *Proc. Natl. Acad. Sci. U.S.A.* **2003**, *100*, 8704−8709.

(18) Tomita, A.; Sato, T.; Ichiyanagi, K.; Nozawa, S.; Ichikawa, H.; Chollet, M.; Kawai, F.; Park, S.-Y.; Tsuduki, T.; Yamato, T.; et al. Visualizing Breathing Motion of Internal Cavities in Concert with Ligand Migration in Myoglobin. *Proc. Natl. Acad. Sci. U.S.A.* **2009**, *106*, 2612−2616.

(19) Petrich, J. W.; Poyart, C.; Martin, J. L. Photophysics and Reactivity of Heme Proteins: A Femtosecond Absorption Study of Hemoglobin, Myoglobin, and Protoheme. *Biochemistry* **1988**, *27*, 4049−4060.

(20) Lepeshkevich, S. V.; Stasheuski, A. S.; Parkhats, M. V.; Galievsky, V. A.; Dzhagarov, B. M. Does Photodissociation of Molecular Oxygen from Myoglobin and Hemoglobin Yield Singlet Oxygen? *J. Photochem. Photobiol. B: Biol.* **2013**, *120*, 130−141.

(21) Andrest, S. F.; Atassi, M. Z. Conformational Studies on Modified Proteins and Peptides. Artificial Myoglobins Prepared with Modified and Metalloporphyrins. *Biochemistry* **1970**, *9*, 2268−2275.

(22) Feitelson, J.; Spiro, T. G. Bonding in Zinc Proto- and Mesoporphyrin Substituted Myoglobin and Model Compounds Studied by Resonance Raman Spectroscopy. *Inorg. Chem.* **1986**, *25*, 861−865.

(23) Shibata, Y.; Kurita, A.; Kushida, T. Real-Time Observation of Conformational Fluctuations in Zn-Substituted Myoglobin by Time-Resolved Transient Hole-Burning Spectroscopy. *Biophys. J.* **1998**, *75*, 521−527.

(24) Shibata, Y.; Ishikawa, H.; Takahashi, S.; Morishima, I. Time-Resolved Hole-Burning Study on Myoglobin: Fluctuation of Restricted Water within Distal Pocket. *Biophys. J.* **2001**, *80*, 1013−1023.

(25) Antonini, E.; Brunori, M. *Hemoglobin and Myoglobin in Their Reaction with Ligands*; North-Holland Publishers Co.: Amsterdam, 1971.

(26) Teale, F. W. J. Cleavage of the Haem−Protein Link by Acid Methylethylketone. *Biochim. Biophys. Acta* **1959**, *35*, 543.

(27) Shosheva, A. Ch.; Christova, P. K.; Atanasov, B. P. pH-Dependence of Photo-Induced Electron Transfer in Zinc-Substituted Sperm Whale Myoglobin. *Biochim. Biophys. Acta* **1988**, *957*, 202−206.

(28) Zenkevich, E.; Sagun, E.; Knyukshto, V.; Shulga, A.; Mironov, A.; Efremova, O.; Bonnett, R.; Songca, S. P.; Kassem, M. Photophysical and Photochemical Properties of Potential Porphyrin and Chlorin Photosensitizers for PDT. *J. Photochem. Photobiol. B* **1996**, *33*, 171−180.

(29) Gradyushko, A. T.; Tsvirko, M. P. Probabilities of Intercombination Transitions in Porphyrin and Metalloporphyrin Molecules. *Opt. Spectrosc. (USSR)* **1971**, *31*, 291−295.

(30) Dzhagarov, B. M.; Lepeshkevich, S. V. Kinetic Studies of Differences between α- and β-Chains of Human Hemoglobin: An Approach for Determination of the Chain Affinity to Oxygen. *Chem. Phys. Lett.* **2004**, *390*, 59−64.

(31) Lepeshkevich, S. V.; Dzhagarov, B. M. Mutual Effects of Proton and Sodium Chloride on Oxygenation of Liganded Human Hemoglobin: Oxygen Affinities of the α and β Subunits. *FEBS J.* **2005**, *272*, 6109−6119.

(32) Lepeshkevich, S. V.; Dzhagarov, B. M. Effect of Zinc and Cadmium Ions on Structure and Function of Myoglobin. *Biochim. Biophys. Acta* **2009**, *1794*, 103−109.

(33) Lepeshkevich, S. V.; Parkhats, M. V.; Stepuro, I. I.; Dzhagarov, B. M. Molecular Oxygen Binding with α and β Subunits within the R Quaternary State of Human Hemoglobin in Solutions and Porous Sol−Gel Matrices. *Biochim. Biophys. Acta* **2009**, *1794*, 1823−1830.

(34) Lepeshkevich, S. V.; Konovalova, N. V.; Dzhagarov, B. M. Laser Kinetic Studies of Bimolecular Oxygenation Reaction of α and β Subunits within the R State of Human Hemoglobin. *Biochem. (Russian)* **2003**, *68*, 676−685.

(35) Papp, S.; Vanderkooi, J. M.; Owen, C. S.; Holtom, G. R.; Phillips, C. M. Reactions of Excited Triplet States of Metal Substituted Myoglobin with Dioxygen and Quinone. *Biophys. J.* **1990**, *58*, 177−186.
(36) Albani, J.; Alpert, B. Fluctuation Domains in Myoglobin Fluorescence Quenching Studies. *Eur. J. Biochem.* **1987**, *162*, 175−178.
(37) Luo, L.; Chang, Ch.-H.; Chen, Y.-Ch.; Wu, T.-K.; Diau, E. W.-G. Ultrafast Relaxation of Zinc Protoporphyrin Encapsulated within Apomyoglobin in Buffer Solutions. *J. Phys. Chem. B* **2007**, *111*, 7656−7664.
(38) Knyukshto, V. N.; Shulga, A. M.; Sagun, E. I.; Zenkevich, E. I. Extra-Liganding Effects in Zn-Octaethylporphyrin Solutions in a Temperature Interval of 300−77 K. *J. Appl. Spectrosc.* **1998**, *65*, 943−951.
(39) Dzhagarov, B. M.; Salokhiddinov, K. I.; Egorova, G. D.; Gurinovich, G. P. Effectiveness of the Formation of Singlet Oxygen Photosensitised by Water-Soluble Porphyrins. *Russ. J. Phys. Chem.* **1987**, *61*, 1281−1283.
(40) Ganzha, V. A.; Gurinovich, G. P.; Dzhagarov, B. M.; Egorova, G. D.; Sagun, E. I.; Shulga, A. M. Influence of the Molecular Structure on the Quenching of Triplet States of Porphyrins by Molecular Oxygen. *J. Appl. Spectrosc.* **1989**, *50*, 402−406.
(41) Bachilo, S. M.; Weisman, R. B. Determination of Triplet Quantum Yields from Triplet−Triplet Annihilation Fluorescence. *J. Phys. Chem. A* **2000**, *104*, 7711−7714.
(42) Zemel, H.; Hoffman, B. M. Long-Range Triplet−Triplet Energy Transfer within Metal-Substituted Hemoglobins. *J. Am. Chem. Soc.* **1981**, *103*, 1192−1201.
(43) Barboy, N.; Feitelson, J. Quenching of Zinc-Protoporphyrin Triplet State as a Measure of Small-Molecule Diffusion through the Structure of Myoglobin. *Biochemistry* **1987**, *26*, 3240−3244.
(44) Barboy, N.; Feitelson, J. Diffusion of Small Molecules through the Structure of Myoglobin. Environmental Effects. *Biochemistry* **1989**, *28*, 5450−5456.
(45) Ye, X.; Demidov, A.; Champion, P. M. Measurements of the Photodissociation Quantum Yields of MbNO and MbO_2 and the Vibrational Relaxation of the Six-Coordinate Heme Species. *J. Am. Chem. Soc.* **2002**, *124*, 5914−5924.
(46) Dzhagarov, B. M.; Galievsky, V. A.; Kruk, N. N.; Yakutovich, M. D. Photodissociation of Oxygenated Forms of the Native Hemoglobin HbA and Its Isolated α- and β-Subunits and Kinetics of Molecular Oxygen Rebinding. *Dokl. Biophys. (Dokl. Akad. Nauk)* **1999**, *366*, 38−41.
(47) Scott, E. E.; Gibson, Q. H. Ligand Migration in Sperm Whale Myoglobin. *Biochemistry* **1997**, *36*, 11909−11917.
(48) Frederiksen, P. K.; Mcllroy, S. P.; Nielsen, C. B.; Nikolajsen, L.; Skovsen, E.; Jørgensen, M.; Mikkelsen, K. V.; Ogilby, P. R. Two-Photon Photosensitized Production of Singlet Oxygen in Water. *J. Am. Chem. Soc.* **2005**, *127*, 255−269.
(49) Baier, J.; Fuβ, T.; Pöllmann, C.; Wiesmann, C.; Pindl, K.; Engl, R.; Baumer, D.; Maier, M.; Landthaler, M.; Bäumler, W. Theoretical and Experimental Analysis of the Luminescence Signal of Singlet Oxygen for Different Photosensitizers. *J. Photochem. Photobiol. B: Biol.* **2007**, *87*, 163−173.
(50) McNaughton, L.; Hernández, G.; LeMaster, D. M. Equilibrium O_2 Distribution in the Zn^{2+}-Protoporphyrin IX Deoxymyoglobin Mimic: Application to Oxygen Migration Pathway Analysis. *J. Am. Chem. Soc.* **2003**, *125*, 3813−3820.
(51) Michaeli, A.; Feitelson, J. Reactivity of Singlet Oxygen toward Amino Acids and Peptides. *Photochem. Photobiol.* **1994**, *59*, 284−289.
(52) Lindig, B. A.; Rodgers, M. A. J. Rate Parameters for the Quenching of Singlet Oxygen by Water-Soluble and Lipid-Soluble Substrates in Aqueous and Micellar Systems. *Photochem. Photobiol.* **1981**, *33*, 627−634.
(53) Matheson, I. B. C.; Etheridge, R. D.; Kratowich, N. R.; Lee, J. The Quenching of Singlet Oxygen by Amino Acids and Proteins. *Photochem. Photobiol.* **1975**, *21*, 165−171.
(54) Krasnovsky, A. A., Jr.; Venediktov, E. A.; Chernenko, O. M. Quenching of Singlet Oxygen by the Chlorophylls and Porphyrines. *Biophysics* **1982**, *27*, 1009−1016.
(55) Schmidt, R.; Shafii, F.; Hild, M. The Mechanism of the Solvent Perturbation of the $a^1\Delta_g \rightarrow X^3\Sigma_g^-$ Radiative Transition of O_2. *J. Phys. Chem. A* **1999**, *103*, 2599−2605.
(56) Scurlock, R. D.; Ogilby, P. R. Effect of Solvent on the Rate Constant for the Radiative Deactivation of Singlet Molecular Oxygen ($^1\Delta_gO_2$). *J. Phys. Chem.* **1987**, *91*, 4599−4602.
(57) Scurlock, R. D.; Nonell, S.; Braslavsky, S. E.; Ogilby, P. R. Effect of Solvent on the Radiative Decay of Singlet Molecular Oxygen ($a^1\Delta_g$). *J. Phys. Chem.* **1995**, *99*, 3521−3526.
(58) Hild, M.; Schmidt, R. The Mechanism of the Collision-Induced Enhancement of the $a^1\Delta_g \rightarrow X^3\Sigma_g^-$ and $b^1\Sigma_g^+ \rightarrow a^1\Delta_g$ Radiative Transitions of O_2. *J. Phys. Chem. A* **1999**, *103*, 6091−6096.
(59) Dzhagarov, B. M.; Jarnikova, E. S.; Stasheuski, A. S.; Galievsky, V. A.; Parkhats, M. V. Effect of Medium Dielectric Properties on Spontaneous Emission of Molecular Singlet Oxygen. *J. Appl. Spectrosc.* **2013**, *79*, 861−865.
(60) Babul, J.; Stellwagen, E. Measurement of Protein Concentration with Interferences Optics. *Analyt. Biochem.* **1969**, *28*, 216−221.
(61) Jensen, R. L.; Holmegaard, L.; Ogilby, P. R. Temperature Effect on Radiative Lifetimes: The Case of Singlet Oxygen in Liquid Solvents. *J. Phys. Chem. B* **2013**, *117*, 16227−16235.